THE CHEMICAL SYNTHESIS AND CHARACTERIZATION OF A CELLULOSE DERIVATIVE

Lappeenranta–Lahti University of Technology LUT

MSc in Biorefineries

2024

Mira Kärkkäinen

Examiner: Prof. Tuomo Sainio

Supervisors: Assistant prof. Rama Layek

Harri Kosonen, D. Sc.

ABSTRACT

Lappeenranta–Lahti University of Technology LUT

LUT School of Engineering Science

Chemical Engineering

Mira Kärkkäinen

THE CHEMICAL SYNTHESIS AND CHARACTERIZATION OF A CELLULOSE DERIVATIVE

Master's thesis

2024

75 pages, 41 figures, 10 tables and 3 appendices

Examiner: Professor Tuomo Sainio

Keywords: Cellulose chemical modification; cellulose dissolution; cellulose carbamate; carbamation reaction; FTIR-ATR; autohydrolysis

Cellulose carbamation is a chemical modification method which facilitates dissolution in a cold NaOH solvent and subsequent regeneration into products such as films or textile fibers. Typically, the carbamation reaction starts from urea which is decomposed in a high temperature and generates isocyanic acid. It reacts with cellulose hydroxyl groups forming cellulose carbamate. Additional drying and/or washing steps can be involved.

In this thesis, a couple distinctive carbamation methods were studied to assess their applicability and scalability. The first method was a hot press which is typically used in the plywood and textile industries. The second method was a closed reactor which provided an opportunity to prevent the gaseous reactant from escaping the reaction environment.

The hot press carbamation turned out to produce a material with the desired extent of carbamation and other properties. The reaction time was in the scale of minutes, which makes the hot press an attractive method. The closed reactor produced a carbamated product which was also hydrolyzed to a significant extent. The hydrolysis had a high effect on the level of carbamation.

In addition, the carbamated products were characterized by nitrogen content analysis and FTIR-ATR to compare the methods in determining the degree of substitution. FTIR-ATR was not able to accurately analyze the DS on all samples – however, there were significant differences between samples carbamated on different methods.

TIIVISTELMÄ

Lappeenrannan–Lahden teknillinen yliopisto LUT

LUT Teknis-luonnontieteellinen

Kemiantekniikka

Mira Kärkkäinen

SELLULOOSAJOHDANNAISEN KEMIALLINEN SYNTEESI JA KARAKTERISOINTI

Kemiantekniikan diplomityö

2024

75 sivua, 41 kuvaa, 10 taulukkoa ja 3 liitettä

Tarkastaja: Professori Tuomo Sainio

Avainsanat: Selluloosan kemiallinen muokkaus, selluloosan liuotus, selluloosakarbamaatti, karbamointi, FTIR-ATR, autohydrolyysi

Selluloosan karbamointi on kemiallisen muokauksen menetelmä, joka mahdollistaa selluloosan liuotuksen kylmään NaOH-liuottimeen, sekä regeneroinnin tuotteiksi, kuten filmeiksi tai tekstiilikuiduiksi. Tyypillisesti karbamointireaktion lähtöaine on urea, joka hajoaa korkeassa lämpötilassa tuottaen isosyaanihappoa. Se reagoi selluloosan hydroksyyliryhmien kanssa tuottaen selluloosakarbamaattia. Prosessissa voi olla myös lisäksi pesu- tai kuivausvaiheita.

Tässä diplomityössä tutkitaan muutamaa erilaista karbamointimetodia, jotta niiden soveltuvuutta ja skaalattavuutta voitaisiin arvioida. Ensimmäinen metodi oli kuumaprässi, jota tyypillisesti käytetään vaneri- ja tekstiiliteollisuudessa. Toinen metodi oli suljettu reaktori, joka esti kaasumaista reaktanttia karkaamasta reaktioympäristöstä.

Kuumaprässikarbamointi tuotti materiaalin, jolla oli haluttu karbamointiaste ja muut ominaisuudet. Reaktioaika oli minuuttien luokkaa, joka tekee kuumaprässistä houkuttelevan metodin. Suljettu reaktori tuotti karbamoidun tuotteen, joka oli hydrolysoitunut merkittävästi. Hydrolyysilla oli suuri vaikutus karbamointiasteeseen.

Lisäksi, karbamoidut tuotteet karakterisoitiin typpipitoisuusanalyysilla ja FTIR-ATR:llä, jotta metodeja voitiin verrata substituutioasteen määrittämisessä. FTIR-ATR ei pystynyt analysoimaan substituutioastetta tarkasti kaikilla näytteillä – kuitenkin, eri metodeilla karbamoitujen näytteiden välillä oli merkittäviä eroja.

ACKNOWLEDGEMENTS

I want to say huge thanks to anyone who was part of my thesis process – whether directly or indirectly. First my examiner and supervisors – including Sakari who was a great back-up and support in brainstorming among other things. Also, anyone at UPM who was part of my project in one way or another, whether big or small – the researchers, laborants and operators. And not to forget my awesome office-mates and fellow thesis workers Wilma and Milla! Moreover, I was hugely supported in other areas of life, too, by my family and friends, including Masi the dog. All of you also deserve my heartfelt thanks for taking me through this life stage and always being there for me.

SYMBOLS AND ABBREVIATIONS

Symbols

a*	CIELAB green-red coordinate	[-]
b*	CIELAB blue-yellow coordinate	[-]
c	mass fraction of urea in impregnation liquid	[%]
DMC	dry matter content	[%]
L*	CIELAB white-black coordinate	[-]
m_{dry}	mass of pulp sheet after impregnation	[g]
M_N	molar mass of nitrogen	[g/mol]
m_{pulp}	mass of pulp	[g]
m_{urea}	mass of urea	[g]
M_{urea}	molar mass of urea	[g/mol]
m_{wet}	mass of pulp sheet after impregnation	[g]
N%	nitrogen content	[%]
ΔE	CIELAB color difference	[-]
w_{urea}	urea mass fraction per cellulose	[%]

Abbreviations

AGU	anhydroglucose unit
ATR	attenuated total reflectance
CA	cellulose acetate
CC	cellulose carbamate
CED	cuprimethylenediamine

D	dried
DP	degree of polymerization
DS	degree of substitution
FTIR	Fourier-transform infrared spectroscopy
HNCO	isocyanic acid
HP	hot press
LHW	liquid hot water treatment
MCC	microcrystalline cellulose
ND	never-dried
NMMO	N-Methylmorpholine N-oxide
RO	reverse osmosis
SA	sodium acetate
TG	thermogravimetric analysis
ZC	zinc chloride
ZS	zinc sulphate

Table of contents

Abstract

Acknowledgements

Symbols and abbreviations

1 Introduction 10
I. Literature part 13
2 Cellulose 13
2.1 Structure and properties 13
2.2 Accessibility, reactivity and solubility 15
2.3 Cellulosic pulps 17
3 Regenerated textile fibers 18
3.1 Viscose 18
3.2 Cellulose acetate 19
3.3 Lyocell 19
3.4 Regenerated products 20
4 Cellulose carbamate 21
4.1 Urea 22
4.2 HNCO reactions 23
4.3 Reactions between cellulose and urea 25
4.4 Quality and characterization 26
4.4.1 Nitrogen content and degree of substitution 26
4.4.2 Discoloration of pulps 26
4.4.3 Color measurements 27
5 Overview of carbamation methods 28
5.1 Raw materials 29
5.1.1 Never-dried pulp 30
5.2 Pretreatment 30
5.3 Impregnation and reaction 32
5.3.1 Catalysts 34

5.4 Washing....34
6 Dissolution of cellulose and its derivatives in cold alkali....34
6.1 General aspects....35
6.2 Carbamate dissolution in NaOH....36
II. Experimental part....37
7 Structure and objective of the experimental part....37
8 Materials and methods....38
8.1 Materials....38
8.2 Methods....39
8.2.1 Impregnation....39
8.2.2 Carbamation....40
8.2.3 Washing....42
8.3 Thermogravimetric analyses....43
8.4 Characterization of products....43
8.4.1 FTIR-ATR....45
8.5 Dissolution....46
9 Results and discussion....47
9.1 Thermogravimetric analyses....47
9.2 Starting materials....48
9.3 Preliminary testing and dissolutions....49
9.4 Hot press....50
9.4.1 Impregnations....50
9.4.2 Carbamations....51
9.4.3 Analysis of effects....53
9.5 Closed reactor....54
9.5.1 Never dried versus dried....54
9.5.2 Catalyst screening....58
9.5.3 Carbamation....60
9.6 Oven carbamation....63
9.7 Washing test....64
9.1 FTIR-ATR....66
9.2 Color and whiteness of the samples....70
Conclusions....73

References.....76

Appendices

Appendix 1. Measurement data

Appendix 2. Main effects plots

Appendix 3. Regression models

1 Introduction

Cellulose is well known for being an abundant, renewable and versatile material for numerous products which are staples in society. For decades, it has been the main material of paper and cardboard products, as well as textiles. Cellulosic textile fibers have unique moisture management and absorbency features, which facilitate wearing comfort. Therefore, they have not been completely replaced by low-cost synthetic fibers, such as polyamide and polyester. (Mendes et al., 2021)

Cellulose is present in all plants, but the cellulose content of different plant origins varies greatly: for example cotton linters have a cellulose content up to 95-99 %, whereas wood plants have a cellulose content of 40-50 %. Due to its high cellulose content, cotton can be utilized in natural textile fibers with minimal processing and good properties. However, due to the highly negative environmental impact of cotton production, as well as low production rates, an increase in the demand for man-made fibers is expected. (Mendes et al., 2021; Sayyed et al., 2019)

In fact, the overall textile product demand is growing worldwide, and therefore also the associated environmental and social impacts, summarized in figure 1. Beginning from the land and water use when cultivating feedstocks, cotton is especially fresh water-intensive. The use of toxic chemicals in production processes is associated with health hazards and pollution especially in developing countries, where a major part of production is centered. Synthetic fibers are energy-intensive and accompanied by microplastics release throughout their life cycle, as well as becoming plastic waste. In addition to the environmental impacts, negative social impacts such as forced and child labor are associated with textile production.

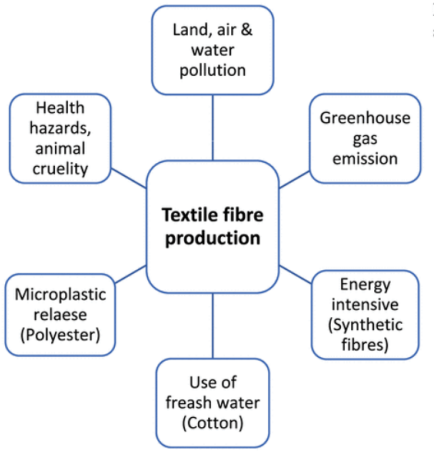

Figure 1. A summary of environmental and social effects of textile fibers (Nayak, 2022).

Man-made cellulosic fibers can offer the desirable properties of natural fibers without some of the drawbacks, such as high water use and high cost. Viscose is currently the most prevalent regenerated man-made fiber technology worldwide. Unfortunately, the viscose process is strongly associated with environmental and technical concerns due to the use of hazardous CS_2 and strongly alkaline and acidic conditions. (Mendes et al., 2021) Consequently, many developed countries have withdrawn from the viscose fiber industry in the recent years, shifting the focus of the production to Asia. (NASDAQ, 2019)

Alternatives to viscose have been under development for decades, but recently many processes have gained interest and momentum. Only in Finland, several environmentally friendly man-made textile fiber products are emerging. Processes include for example ionic liquids, enzymes and cellulose carbamate (CC). The latter, based on the reaction of cellulose and urea in a high temperature, has been known for decades but no successful full-scale production has developed. Currently, Infinited Fiber Company is close to commercialization with their cellulose carbamate produced from recycled textiles. (Suomen Tekstiili & Muoti, 2021)

A key advantage of CC compared to viscose is that the intermediate product, *i.e.* the modified pulp, can be stored for long times and transported once dried. Drying takes a significant amount of energy, and on top of that, man-made fibers overall are characterized by a high energy consumption. (Nayak, 2022) Therefore, energy savings are of high importance for the sustainability and economy of the process. The energy required for drying can be saved if the production facility is integrated to a pulp mill. The integration, along with chemical recycling, is the most efficient way to reduce the carbon footprint of the cellulose carbamate

fibers. (Paunonen et al., 2019) Further savings can be brought by reducing the need for heat and chemicals in the carbamate production, for example in the drying and reaction steps.

This Master's thesis is focused on the cellulose carbamation process. Its aim is to study different reaction environments and conditions, keeping scalability in mind. The effect of the varying conditions on the properties of the final product will be studied, accompanied by the product's processability for subsequent process steps. In addition, some characterization aspects will be studied.

- What is the effect of water content on the extent of the reaction?
- How does reducing the number of drying cycles affect the extent of the reaction?
- What is the effect of a closed reaction environment on the extent of the reaction and the product?
- How does the heating method affect the extent of the reaction?
- Could certain catalysts have a positive effect on the extent of the reaction or properties of the final material?

I. Literature part

2 Cellulose

Cellulose is the most abundant polymeric material found on earth, as well as the most common substance in nature. In lignocellulosic biomass, it is present in the plant cell wall along with hemicellulose and lignin. The structural hierarchy from the wood tissue to the molecular level is presented in figure 2. In hardwoods and softwoods, cellulose consists about 40-50% of the plant mass. Once isolated by pulping, cellulose can be processed into various materials and products. The properties of cellulose depend strongly on its molecular, supramolecular and morphological structure (Wertz et al., 2010)

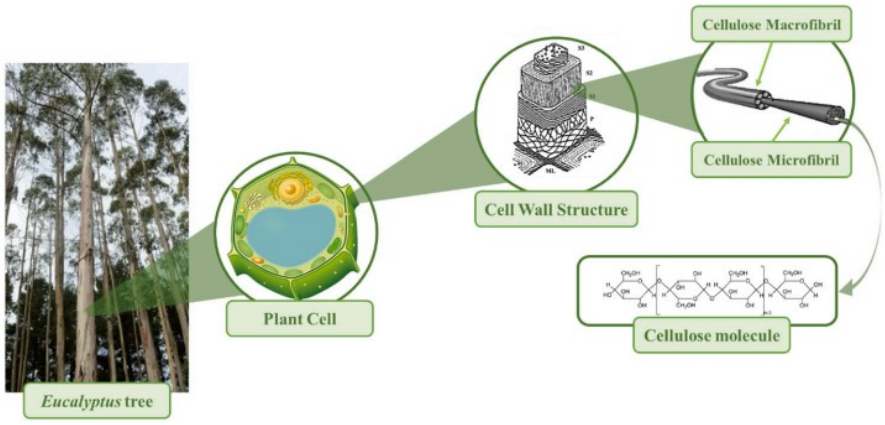

Figure 2. Structural hierarchy from wood plant to cellulose molecule (Mendes et al., 2021).

2.1 Structure and properties

On the molecular level, cellulose is a polymer composed of repeating D-glucopyranose molecules. The molecular structure is presented in figure 3. These anhydroglucose (AGU) units form a linear covalently linked polymer chain. The amount of AGU units in a cellulose chain is described by the degree of polymerization (DP). In native plant fibers, the DP value is typically between 800-10 000, whereas in technical wood pulp it is between 300-1700. Each AGU unit contains a 6-membered carbon ring where the carbons are identified as C1-C6. In the carbon positions C2, C3 and C6, a hydroxyl (-OH) group is attached. The C1

hydroxyl end of the cellulose chain has a reducing character, and is therefore called the reducing end, whereas the other end is the non-reducing end. (Klemm et al., 2005, Sixta, 2008)

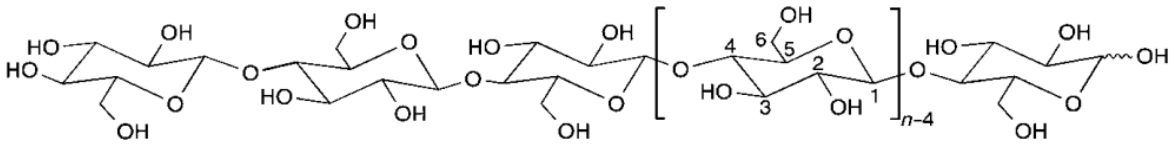

Figure 3. Cellulose molecular structure, including the numbering or carbon sites from C1 to C6. (Klemm et al., 2005).

Due to their chemical composition and conformation, cellulose chains form hydrogen bonding networks intra- and intermolecularly. This forms the smallest supramolecular units, called elementary fibrils or microfibrils depending on the reference. These units form highly ordered crystalline structures as well as less ordered amorphous ones. In fact, the crystalline segments are frequently disrupted by very short rather than wide and bulky amorphous segments. (Kontturi, 2018) The crystallinity of cellulose describes the portion of crystalline regions of the whole structure. The semicrystalline nature of cellulose fibers promotes their mechanical properties and affects their reactivity (Sixta, 2008).

Cellulose solid state crystalline lattice can occur in four (I-IV) distinctive forms, of which the structure I and II have industrial relevance. Cellulose I is the metastable structure in native cellulose. Cellulose I can be irreversibly transformed to cellulose II by treatment with aqueous alkali, or by dissolving and regenerating the cellulose. The hydrogen bonding structure of cellulose I and II are presented in figure 4. (Heinze et al., 2018)

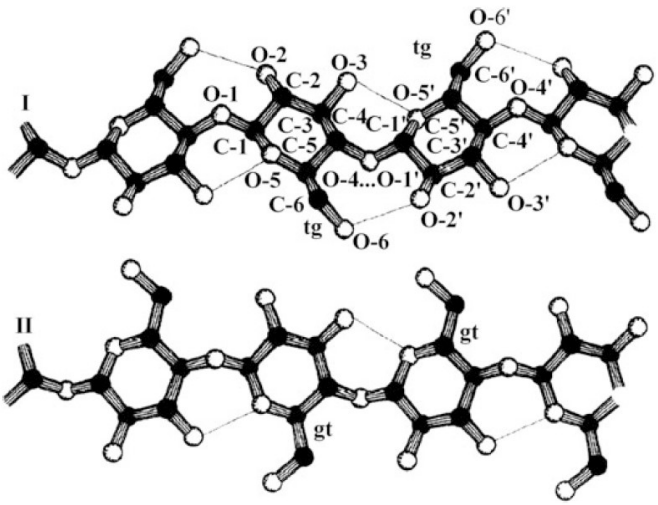

Figure 4 Hydrogen bonding in cellulose I and II (Heinze et al., 2018).

As seen in figure 4, ompared to cellulose I, cellulose II has different conformations of the hydroxymethyl groups, as well as less intramolecular hydrogen bonds. Less hydrogen bonds means less crystallinity which means a better accessibility for solvents or reactants. (Heinze et al., 2018)

2.2 Accessibility, reactivity and solubility

It is necessary to define three terms: accessibility, reactivity and solubility. Accessibility is essentially the relative ease by which reactants or solvents can reach the cellulose molecule, and it is dependent on the structural properties of cellulose (Sixta, 2008). The term reactivity or activity intrinsically includes the accessibility of cellulose, but also the reactivity of the OH-groups towards a suitable reactant. In order to have high reactivity, cellulose needs to have an accessible structure and the OH-groups need to react with a suitable substituent. (Ciolacu & Popa, 2010) The term derivatization refers to the replacement of the OH-group with the substituent. Like reactivity, the term solubility is closely related to accessibility, since solvent molecules need to reach or otherwise interact with the cellulose molecules in order to dissolve them. In fact, cellulose is difficult to dissolve in most common solvents due to poor accessibility.

Cellulose accessibility is mainly determined by its structure. Crystallinity causes the cellulose accessibility, and thus reactivity and solubility, to decrease due to strong hydrogen-bonding. The goal of making cellulose more accessible, reactive and soluble (often called activation) is essentially to decrease its crystallinity. (Heinze et al., 2018) A successful activation is essential for cellulose which is intended to be chemically modified. For example, a common activation strategy is mercerization which involves cellulose treatment with aqueous alkali, transforming the crystalline structure from cellulose I to cellulose II.

Hornification is a key phenomenon in pulp processing which decreases cellulose accessibility via crystallization. When thermally dried, the structure of cellulose fibers stiffens and some domains become inaccessible. The fiber properties, such as water retention, *i.e.* swelling, ability deteriorate irreversibly. Therefore never-dried pulp is usually preferred over dried pulp, which is more convenient for transporting in sheet form. The hornification continues even through multiple wetting-drying cycles (Dubowik et al., 2014). A schematic representation of hornification in a cellulose fiber cell is presented in figure 5.

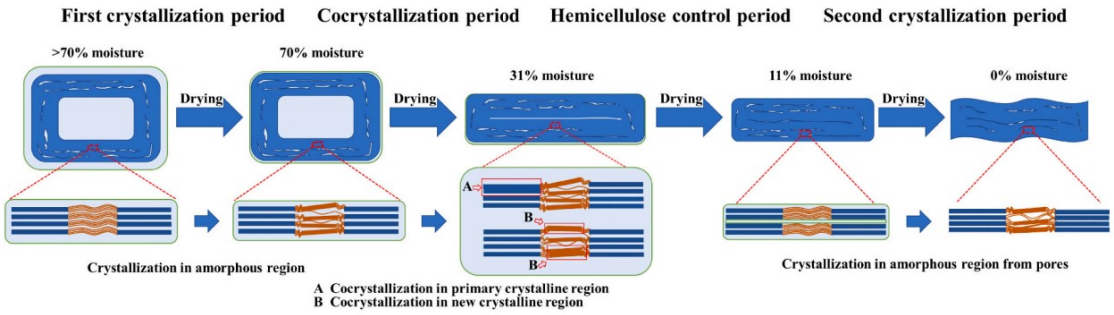

Figure 5 A schematic illustration of the progress of cellulose fiber cell hornification as moisture content decreases (modified from Mo et al., 2022).

In the first stage of figure 5, only interfiber water is removed and the fiber morphology is not affected and hornification does not occur. When moisture content drops below about 75-55%, the water is removed from inside the fiber, collapsing it. Simultaneously, cocrystallization, ie combining of adjacent microcrystals, causes hardening of the fiber. If hemicellulose or lignin are present in the fiber, they slow down the process of hornification. The hemicellulose control period refers to the moisture range where hemicellulose prevents the effect of hornification by swelling. In the final stage below 10 %, the cellulose

crystallizes further, and the pores shrink as water exits them. Finally, the cell wall is hardened and compacted, and can't be fully swollen by water (Mo et al., 2022)

2.3 Cellulosic pulps

Pure cellulose does exist in the nature for example in the form of cotton linters, but it is a marginal group of materials. Most cellulosic materials are obtained through a pulping process which is composed of pulping, bleaching, washing and drying steps. As a result, the cellulose is not completely pure and refined, and the purity can have fundamental effects on subsequent processing.

The purity of cellulose is composed of at least two aspects: other components and chemical changes. The other components include hemicellulose, lignin, extractives and other impurities which are left in the product despite purifying stages. Chemical changes include unintended chain shortening, oxidation and even derivatization of the cellulose hydroxyl groups. (Goto et al., 2021) The oxidation of hydroxyl groups into carbonyl or carboxyl groups occurs not only in isolation and purification processes, but also in the form of natural aging, which is accelerated by *e.g.* heat and light exposure. Oxidation can affect several properties of cellulose, such as yellowing, strength and alkali stability. (Potthast et al., 2006)

There are two major classes of cellulosic pulps: dissolving and paper grade pulps. Dissolving pulps are manufactured mainly for use in the viscose process and chemical modification. Dissolving pulp is composed of more than 90 % pure cellulose, and typically less than 5% hemicellulose. The production methods are mainly acidic sulfite and pre-hydrolysis kraft processes. (Mendes et al., 2021) Further alkali purification can be done if necessary, but it causes a considerable increase in production costs (Sixta, 2008)

Paper grade pulps differ from dissolving pulps by their better mechanical properties in sheet form, and higher alkali resistance. They are typically manufactured by the Kraft pulping method. They have a higher hemicellulose content which leads to lower reactivity and several problems in the viscose process. These include for example decrease of filterability, inhibition of reactions and discoloration. (Sixta, 2008)

3 Regenerated textile fibers

Man-made cellulosic textile fibers are a growing market. The shares of production volumes of different types of man-made cellulosic fibers are presented in figure 6. The markets are dominated by viscose (80 %), followed by acetate (13 %) and Lyocell (4 %) (Textile Exchange, 2023).

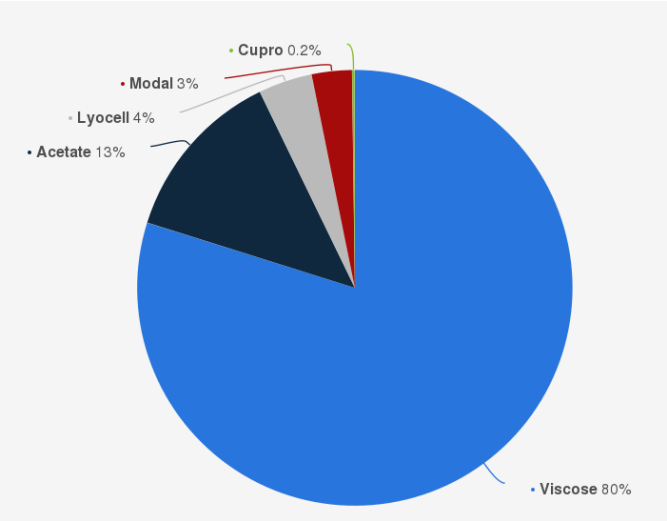

Figure 6 Man-made cellulosic textile fiber production volume by type, worldwide in 2022. (Textile Exchange, 2023).

Viscose and acetate are derivatizing methods in which the cellulose is chemically modified and thereafter dissolved. Lyocell is a non-derivatizing method in which cellulose is directly dissolved in a suitable solvent.

3.1 Viscose

Currently, the most important large-scale cellulose derivative for the production of textile fibers is cellulose xanthogenate (xanthate), which is the starting point of viscose (rayon) fiber and cellophane film production. The chemical modification is necessary to dissolve the cellulose. The modification process starts with steeping the cellulose with 17-19 % NaOH solution and aging the mixture for 4-5 hours. The mixture is reacted with carbon disulphide (CS_2) to form cellulose xanthate, and ripened for 15 hours. Once a dissolved state of the

cellulose is obtained, the solution is filtered to remove undissolved particles and deaerated to remove air bubbles. In the final spinning stage, it is extruded through small holes (*i.e.* a spinneret) into a coagulation bath which contains a mixture of acid and salts. At this stage, the xanthate groups cleave off of the cellulose backbone and the cellulose regenerates into a solid fiber form. (Mendes et al., 2021)

CS_2 along with heavy-metal compounds, strong acids and alkalis, and harmful by-products leads to problematic environmental loads, in the form of both gaseous emissions and waste waters. An alternative to viscose technology should generally be a simpler process, as well as free from environmentally hazardous materials and by-products. (Klemm et al. 2005)

3.2 Cellulose acetate

Cellulose acetate (CA) is one of the oldest derivatizing processes to produce cellulosic textile fibers. CA fibers are mostly produced in the United States. (Sayyed et al., 2019) The derivative is formed from the reaction of cellulose and acetic anhydride - typically in the presence of sulfuric acid as catalyst. Typically, the cellulose hydroxyl groups are first fully substituted and subsequently, part of the substitute groups are hydrolyzed to obtain a uniform product with desired properties. (Heinze et al., 2018)

After derivatization, cellulose acetate is dissolved in a solvent (typically acetone) and the solution is filtered. The solution which contains 25-30 % cellulose acetate, is extruded through the small holes of a spinneret in a countercurrent against hot air, which evaporates the solvent (Woodings, 2001). Cellulose acetate fibers have certain drawbacks which limit their applications: they are poor in fiber strength, abrasion resistance and thermal resistance. They are most typically blended with other fibers in clothing applications that are not worn often. (Sayyed et al., 2019)

3.3 Lyocell

The Lyocell-type process is an example of a non-derivatizing production method for cellulosic man-made textile fibers. It can utilize either an ionic liquid or N-Methylmorpholine N-oxide (NMMO) as the solvent. Ionic liquids are still to overcome

barriers related to high production costs, and are not a commercialized technology as of yet (Sayyed et al., 2019).

After pre-swelling and dissolution, the viscous solution is extruded through spinnerets to form filaments. The extrusion happens in air and the filament passes through an air gap before it is regenerated (*i.e.* the solvent is removed) in a bath. This type of spinning is called dry-jet wet spinning. The solvent can typically be recovered almost completely. The process has the advantages of being simple and eco-friendly. Some disadvantages for NMMO-based process include side-reactions, thermal instability and rather high temperatures in dissolution. (Mendes et al., 2021) A typical temperature for dissolution in NMMO is 120 °C (Sayyed et al., 2019).

3.4 Regenerated products

When cellulose has been successfully and completely dissolved in a solvent, it can be regenerated into the physical forms of products. These include for example fibers, nanoparticles, films and nonwoven mats. (El Seoud et al., 2020)

Man-made cellulosic textile fibers have a wide range of properties and structures. For instance, the fibers can differ in their cross-sectional shape or physical properties, such as density, moisture absorption and tensile strength. (Woodings, 2001) An example of different fiber cross-sections from the viscose, lyocell and carbamate processes is presented in figure 7.

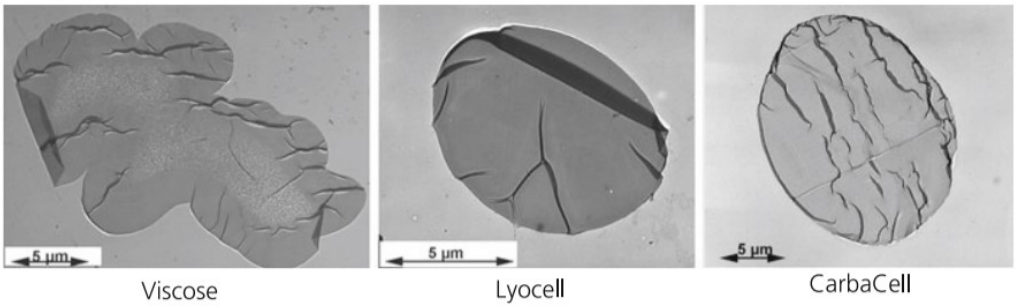

Figure 7 Ultra-thin cross sections of man-made cellulosic fibers from different processes micrographed with transmission electron microscopy (Fink et al., 2014).

Another major regenerated cellulose application is films. Cellophane, also known as viscose films, are one of the oldest packaging materials, and despite the rise of fossil-based

polyolefin films, it still finds applications in *e.g.* sausage casings and membranes. NMMO films have been researched as a promising alternative for the more complicated and environmentally harmful viscose process. Key properties of cellulosic films include for instance transparency, thickness, and permeability properties. (Fink et al., 2014)

The properties of the regenerated products are dependent on the cellulose properties, such as DP, as well as the process parameters, for example during spinning. Another important process step is the dissolution, which can be improved by a suitable cellulose derivatization step.

4 Cellulose carbamate

Cellulose carbamate (CC), sometimes called cellulose aminomethanate, is a carbamic acid ester of cellulose. It is formed from the reaction of urea and cellulose OH-groups in high temperature. The reaction has been reported by several articles. In 1937, Hill and Jacobson patented an early invention in the United States, and ever since there have been several attempts to improve and commercialize the process. (Harlin, 2019)

Cellulose carbamate is a derivatizing process route which bears similarities to viscose technology in many aspects. Their substituted groups are presented in figure 8.

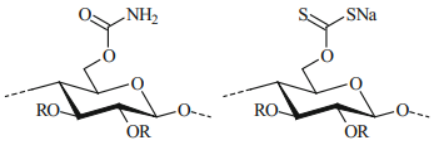

Figure 8 AGU unit structure of cellulose carbamate (left) and cellulose xanthate (right). (Heinze et al., 2018).

In both processes, the starting material is pre-treated, derivatized and dissolved in a sodium hydroxide solution. The solution is filtered, deaerated and subsequently processed into products, such as spun into fibers. The comparison of the steps in a viscose process and a typical CC process is presented in figure 9.

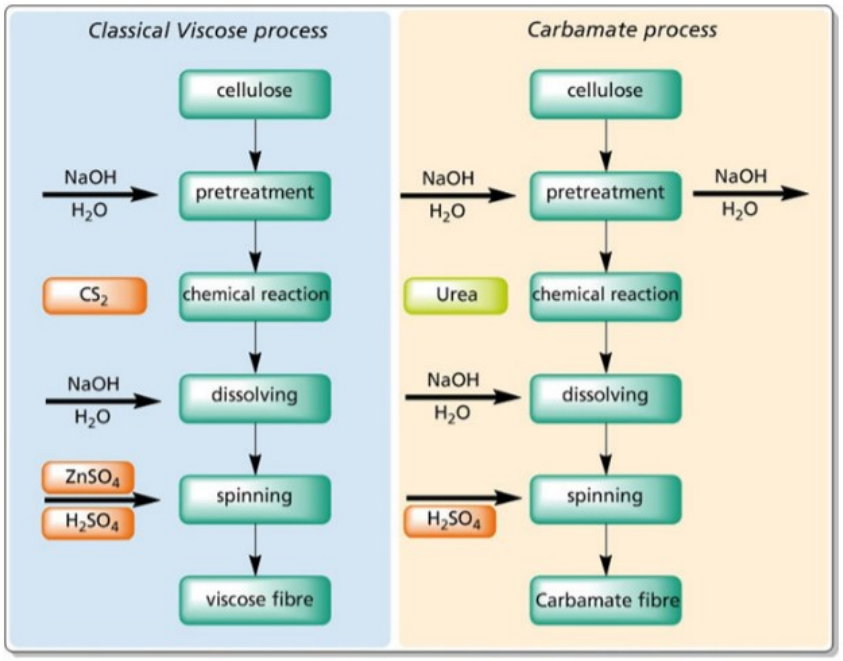

Figure 9. The viscose and the carbamate fiber process. (Fink et al., 2014) For the latter it should be noted that the chemicals and methods can vary significantly, especially in the pretreatment and spinning stages.

The advantages of CC compared to viscose include the absence of toxic CS_2 and better stability of the derivatized pulp. (Klemm et al., 2005) Unlike viscose, CC solution does not need ripening prior to spinning, and thus it can be started immediately after filtering and deaeration (Harlin, 2019). The final CC fiber products have shown properties that are comparable to viscose fibers, as well as better dyeability (Fu et al., 2014). All these factors make cellulose carbamate an attractive alternative to the conventional viscose process.

4.1 Urea

Urea, also known as carbamide, is an organic compound with the molecular formula NH_2CONH_2 and a melting point of 132,7 ˚C. Pure urea is a white, odorless, crystalline solid. It was first synthesized by Friedrich Wöhler in 1828, and nowadays it can be synthesized from ammonia and carbon dioxide. Global urea production capacity is around 220 million tons per year, which is mainly due to its use as a fertilizer. In fact, it is the most nitrogen-rich industrial chemical after ammonia. (American Chemical Society, 2021)

According to Schaber et al. (2004), when heated, the mass loss of dry urea begins at approximately 140 ˚C and continues until approximately 152 ˚C as primarily vaporization. At the range of 152-160 ˚C, a more significant mass loss is observed. This mass loss is attributed to continued vaporization as well as urea decomposition according to equation 1. The products of this decomposition are ammonia and isocyanic acid gases. Isocyanic acid further reacts with cellulose to form cellulose carbamate, and is therefore the desired decomposition product.

$$H_2N\text{-}CO\text{-}NH_2(m) + heat \rightarrow NH_4^+NCO^- \rightarrow NH_3(g) + HNCO(g) \quad (1)$$

Zhu et al. (2021) studied the pyrolysis of urea at constant temperatures, and also found that urea mass loss was mostly due to evaporation in the temperature of 140 ˚C. At 160 ˚C, isocyanic acid and ammonia were released, but isocyanic acid polymerized into cyanuric acid, and was detected in lower amount than in 140 ˚C. Temperatures in excess of 180 ˚C generated isocyanic acid on a higher rate, but they are unfortunately not applicable for cellulose carbamation reactions, since cellulose discolorisation and carbonization are enhanced at these temperatures. Thus, the optimal temperature to decompose urea seems to be at around 140-155 ˚C.

4.2 HNCO reactions

Isocyanic acid, HNCO, is formed from the pyrolytic decomposition of urea and many other N-containing materials. HNCO is known to react with functional groups which contain an "active hydrogen" which is attached to an O, N or S atom. The reaction is a simple addition of the active hydrogen to the N=C bond in HNCO. (Roberts & Liu, 2019) In the cellulose carbamation system, there are several possible reactions of HNCO, including reactions with cellulose, water, ammonia, urea and carbamate. All these reactions, presented in figure 10 and numbered 2-9, make the system quite complex.

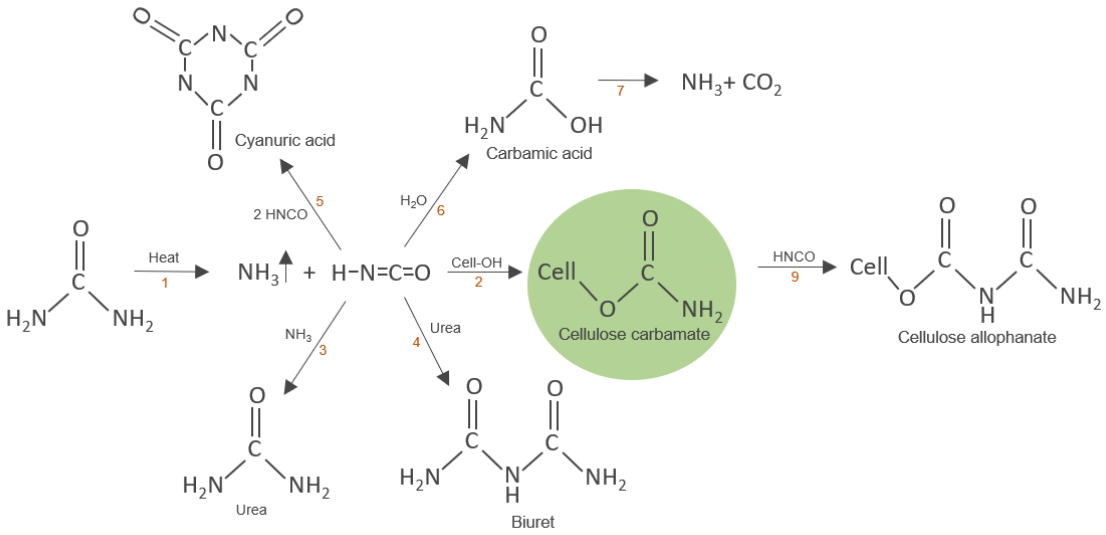

Figure 10. Formation of cellulose carbamate and the side reactions involving isocyanic acid relevant to a temperature range under 190 C. Modified from (Redemann et al., 1958) & (Woodings, 2001).

HNCO is known to react with alcohols, giving carbamates. The equation and mechanism applies also to cellulose -OH groups, presented as reaction 2. The carbamation reaction is parallel to catalyst-free urethane bond formation between an isocyanate and an alcohol. The mechanism is presented in figure 11. First, the electrophile (isocyanate) and the nucleophile (alcohol) form a reactant complex. Then, in the transition state (highlighted in green), the N=C=O group bends and activates the carbon for the formation of a new C-O bond. Simultaneously, the H-O bond breaks and the N-H bond forms, leading to the product. (Waleed et al., 2022). This reaction has been utilized, and is still gaining attention, in cellulose derivatization also with other isocyanates - both aliphatic and aromatic as well as mono- and di-isocyanates (Abushammala & Mao, 2019).

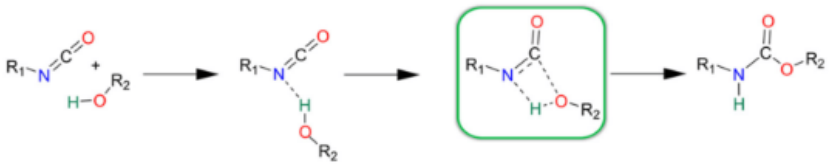

Figure 11. The mechanism of catalyst-free urethane formation. In the case of cellulose carbamate, R_1 = H and R_2 = cellulose. (Waleed et al., 2022).

According to Roberts & Liu (2019), isocyanic acid-alcohol mechanism is the same as the neutral hydrolysis of isocyanic acid with water in solution, depicted as reaction 6. This

reaction yields carbamic acid, which is unstable and decomposes to ammonia and carbon dioxide. Borduas et al. (2016) studied this reaction in conditions which are relative to the atmosphere, and found that the hydrolysis is a relatively slow reaction, resulting in a HNCO lifetime ranging from 10 days to 28 years. However, in high temperatures, the hydrolysis is rapid

HNCO forms biuret when reacting with urea at the temperature range of 152-160 ˚C according to reaction 4. Biuret forms in small amounts during carbamation as an inefficient byproduct (Harlin, 2019). Temperatures in excess of 150-160 ˚C lead to the formation of other byproducts such as cyanuric acid, which can form from either the trimerization of HNCO according to reaction 5, or from triuret. (Schaber et al., 2004).

Another example of this is reaction 3 between HNCO and ammonia in solution, yielding urea. (Roberts & Liu, 2019) In fact, HNCO has been proposed, although not exactly confirmed, to also be reactive towards the NH_2 structure of the carbamate group according to reaction 9, in which case a cellulose allophanate would be formed. (Woodings, 2001)

4.3 Reactions between cellulose and urea

To further complicate the cellulose-urea system, some articles have reported a direct reaction between cellulose and urea. The occurrence of Maillard type reactions betweenthe aldehyde groups in cellulose reducing ends and urea has been proposed by Vo et al. (2014) and Ershova et al. (2012). Maillard type reactions are known in the food and medicine industry as a complex series of browning reactions. Maillard type reactions occur between reducing sugars and free amino acids (or amino derivatives) under heat. The reactions are promoted by alkaline pH and the presence of metal ions. (Crnčević, 2018) Therefore, in suitable conditions, cellulose and urea can possibly react by a condensation reaction, producing a water molecule and an ureide as detected by Ershova et al. (2012), as well as several other products. The reaction is presented as equation 2. (modified from Ershova et al., 2012; Gerrard, 2005)

$$\begin{matrix} R_1 - CO - H \ + \ H_2N - CO - NH_2 \ \leftrightarrows \ R_1 - NH - CO - NH_2 \ + \ H_2O \\ reducing\ end\ sugar\ (aldehyde) + \ urea \ \leftrightarrows \ ureide \ + \ water \end{matrix} \qquad (2)$$

4.4 Quality and characterization

4.4.1 Nitrogen content and degree of substitution

Cellulose carbamate quality and properties are dependent on its degree of substitution (DS), which is the average number of carbamate groups in an AGU unit. The maximum degree of substitution is 3. DS is an important quality since it affects the dissolution process and the quality of the solution. DS is typically determined by analyzing the nitrogen content of the sample.

In addition to DS calculation, nitrogen content can be utilized to calculate the yield of a reaction, and therefore it is the most important quality which is analyzed in the CC product. Nitrogen content is typically analyzed either with the Kjeldahl method or the CHNS-method. Another method to determine the nitrogen content or DS is FTIR (Fourier Transform Infrared spectroscopy) which has been presented in a few articles. Compared to the elemental analysis methods, FTIR is faster, safer and non-destructive.

In addition to the degree of substitution, the evenness (or unevenness) of substitution is an important parameter that affects the cellulose carbamate properties. Heterogeneity of substitution causes irreproducibility of product characteristics, as well as problems in dissolution such as gel particles which can block nozzles during fiber spinning (Heinze et al., 2018). The evenness of substitution can vary from the scale of which -OH groups positions (C2, C3 and C6) are substituted, up to larger scale heterogeneity in the material. Larger scale heterogeneity can sometimes be observed as variations in color or other properties. However, the smaller scale evenness of substitution in CC is extremely difficult to measure, because the DS is relatively low (Guo et al., 2011).

4.4.2 Discoloration of pulps

The color of a product is often an important quality aspect, especially when talking about consumer textiles. Pulp is prone to yellowing or browning (also called discoloration or brightness reversion) during storage, and the color is easily transferred to the final textile product. Brightness reversion is accelerated by heat, which is unavoidably present in the

carbamation environment. In addition, there are several other factors that contribute: for example, contact with air, chemicals, light and irradiation (Ahn et al., 2019). Typically, high-temperature brightness reversion is more severe in a humid environment compared to dry conditions (Sixta, 2008).

The yellowing and brightness reversion of cellulose is the result of chromophore species generated by condensation reactions. Another participants include carbonyl groups and residual non-cellulosic compounds. (Sixta, 2008) Yellowing has been linked to oxidation phenomena, more specifically the oxidation of cellulose hydroxyl groups at the C2 or C3 to keto groups or C6 hydroxyl groups aldehyde groups, or even further to carboxylic acids. In addition, reducing end groups can oxidize into carboxylic acids, but this reaction becomes important only in the case of hydrolyzed cellulose where the molecule chains have broken and thus reducing ends have multiplied. (Ahn et al., 2019) Furthermore, Maillard type reactions cause browning of the cellulose especially in alkaline conditions and in the presence of metal ions, as discussed in chapter 4.3.

In addition to cellulose, it can't be ignored that impurities, such as lignin, hemicellulose, resins or chemical residues, contribute to discoloration (Ahn et al., 2019). In fact, heat-induced discoloration is particularly attributed to hemicelluloses, uronic acids and carbonyl groups. Hemicelluloses have also been shown to be involved in the discoloration of Lyocell and viscose dopes (Sixta, 2008).

The reactions behind pulp yellowing are accelerated by high temperature conditions. Thus the high temperature required for urea decomposition inevitably causes some yellowing of the pulp. Even if discoloration cannot be completely avoided, its monitoring is useful to find ways to control it. Commonly, color control in the textile industry is conducted by combining visual assessment and color measurements.

4.4.3 Color measurements

In the pulping industry, cellulosic pulps are routinely monitored for their brightness, which is determined as the blue reflectance of light at a wavelength of 457 nm. It is a well established and standardized method to control the color of the product. The advantage of this method is that it gives the result as a single number, but the downside is that it does not

fully correspond to the perception of the human eye. Samples with a similar brightness can still appear different in color.

Pulp product whiteness is a parameter which attempts to measure the color of the product as perceived by the human eye. There have been various attempts to describe a color and match the perceived color and a color measuring system. One of the most common ones is CIELAB, which describes the color in three coordinates: L* for white-black, a* for green-red and b* for yellow-blue. The CIELAB color space is presented in figure 12.

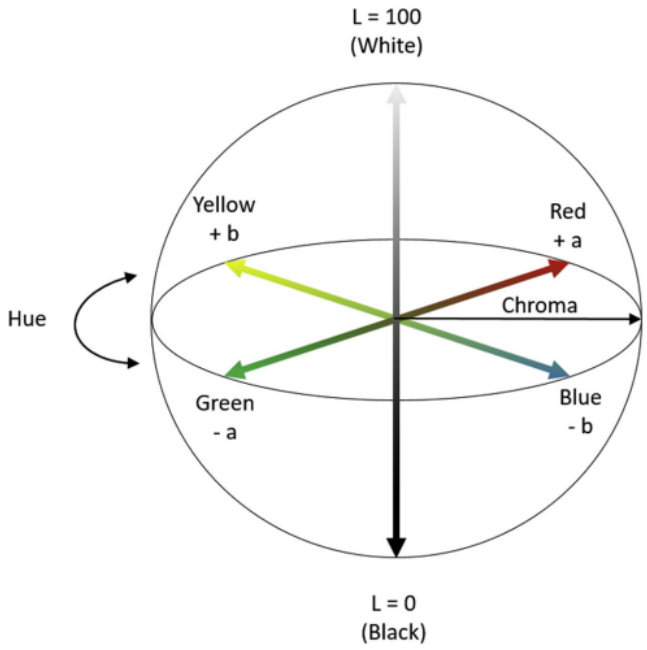

Figure 12. CIELAB color coordinate system (Ly et al., 2020).

The CIELAB system is used in the paper and textile industries to detect changes in color. However, when considering whiteness, challenges arise due to CIELAB being a three-dimensional color space. There are several whiteness formulas which characterize the result in a single number – however, none have been universally agreed upon and still to this day, a brightness measurement is the most typical way to characterize pulp.

5 Overview of carbamation methods

In this chapter, different approaches to the synthesis of cellulose carbamate will be overviewed. Methods which synthesize N-substituted cellulose carbamates will be excluded.

N-substituted carbamates include for example cellulose tricarbanilates which are synthesized with phenyl isocyanate.

The DuPont method from 1937, dubbed “early method” or “conventional method” by Harlin (2019), consists of steeping, pressing, drying, baking and washing. In the steeping phase, urea is introduced into the cellulose as an aqueous solution of at least 15% along with 2-10% sodium hydroxide. The mixture is pressed, dried and baked preferably at 120-150 °C, and subsequently washed. The used baking times ranged from minutes to hours – if the temperature was raised even up to 300 °C, the baking time was reduced to two minutes. (Hill & Jacobson, 1937)

The conventional method is quite simple and requires no special equipment. It involves little harmful or hard to recover substances. Urea is available on a technical scale – however, it is subject to price changes. In 2021-2022, its price more than doubled, rising to an all-time high due to the global pandemic and international conflicts. The price has since returned to the pre-pandemic level. (Kee et al., 2023)

Urea itself is a practically non-hazardous chemical – it produces no direct occupational risk during storage or handling. In addition, it poses no direct harm to the process stages after carbamation. A downside is that the gaseous decomposition products of urea are toxic, which creates an occupational safety concern and sets requirements for *e.g.* ventilation. Ammonia and isocyanic acid are also pollutants which decrease air quality. In addition, the drying and baking in the CC process takes a significant amount of energy.

5.1 Raw materials

A variety of cellulose-containing raw materials have been used for cellulose carbamation. These include a range of softwood, hardwood and non-wood sources such as cotton, bamboo and recycled textiles. Even microcrystalline cellulose (MCC) has been used to produce cellulose carbamate. MCC is produced via acid hydrolysis and has high reactivity and purity. (Kantola et al., 2018)

Wood-derived dissolving pulp is the most typical raw material (Harlin, 2019). Also paper grade pulp has been utilized in carbamation, for example by Hassi and Tikka (2012). In their method, they used alkali treatment to purify the pulp from hemicelluloses. However, kraft

pulp was directly utilized in carbamation by for example Zhang et al. (2013) and Wei et al. (2020). Xu et al. (2023) studied bamboo pulps with different hemicellulose contents and found that increased hemicellulose decreases the reaction yield, as well as solubility and stability of the solution. However, increasing the hemicellulose content from 6 to 16 % was not completely detrimental to the process: for example the solubility decreased only from 98 to 90 %.

5.1.1 Never-dried pulp

Pulp, whether dissolving or paper grade, is most often dried for transportation. In addition, an integrated facility, such as a paper mill, can obtain low-consistency never-dried pulp straight from the pulp mill. This is often beneficial, since as discussed in chapter 2.2, drying deteriorates pulp properties. The benefits of using never-dried pulp for cellulose carbamate are described by Saxell et al. (2014). It was discovered that the accessibility and diffusion of urea in the cellulose fiber increased significantly when using never-dried pulp, resulting in a more efficient reaction.

5.2 Pretreatment

In order to achieve a uniform and high-quality cellulose carbamate, the raw material has to be pre-treated. Activation of the raw material improves reactivity and consequently yield of the carbamation. The main objective of activation is to decrease cellulose crystallinity. Chemical methods activate by swelling or changing the crystalline structure to a more accessible form. Water, organic and dilute solvents increase the surface area by widening pores, cavities and interfibrillar interstices. Concentrated acid or base solutions change the cellulose crystal structure to a more accessible form. (Heinze et al., 2018) Currently the most industrially relevant cellulose activation method is mercerization which involves soaking cellulose in alkali. (Olsson & Westman, 2013; Sixta, 2008)

Cellulose accessibility and reactivity are highly dependent on the degree of polymerization of the cellulose molecule (Heinze et al., 2018). In practice, when cellulose is dissolved the DP needs to be on a low enough level depending on the application. The DP of native cellulose is often very high, but dissolution in aqueous alkali requires a moderately low DP

(Budtova & Navard, 2016). Low DP cellulose molecules dissolve more easily in high concentrations, but the properties of the regenerated products are subsequently compromised. According to Harlin (2019), an optimal DP for CC is at 270-280. Some examples of pretreatment methods used for CC processes are presented in table 1.

Table 1. Examples of pretreatment methods used for cellulose carbamation processes found in literature and patents.

Method	Details	Reference
Radiation	Ionizing electron beam irradiation, energy 10 MeV, dose 10 or 15 kGy	Iller et al., 2007
Steam + acid hydrolysis	Arbron process: Fracturing with steam at 5 bar, 150-160 °C, with sulphuric acid.	Pöyry Finland Oy, 2018
Alkali activation (mercerization)	Not specified	Fink et al., 2014; M. Xu et al., 2021
Hydrothermal treatment	120-160 °C, 0,5-10h, with catalyst	US5906926A
Enzymatic treatment	After mechanical and/or hydrothermal treatment, 20-60 °C for 1 min to 48 h	US5906926A

Activation and depolymerization can be conducted by chemical, mechanical, thermal, enzymatic or radiation methods or their combination. The most typical method in the textile industry is chemical activation by alkali, *i.e.* aqueous NaOH. Mechanical methods include for example grinding or ball mills, and they activate the cellulose by disrupting the fibrillar and crystalline order to some extent (Heinze et al., 2018). In addition, depolymerization can occur if energy is sufficiently high. Mechanical methods have not been studied as much as other processes, since mechanical degradation is not present in a typical pulping process. (Wertz et al., 2010) High-energy radiation is able to activate and depolymerize cellulose, and was applied by Iller et al. (2007) to produce CC as well as other cellulose derivatives.

5.3 Impregnation and reaction

The purpose of impregnation is to transport the urea in contact with the cellulose before carbamation, as well as swell and activate the fiber. Apart from water, various different solvents have been utilized. These include for example inert organic solvents such as xylene, liquid ammonia and supercritical CO2. The latter two require special equipment such as pressure vessels or autoclaves. PEG 2000 and LiCl were also utilized as activation agents.

There have been several attempts to find ways and solvents to perform the carbamation reaction, and they are summarized in table 2. Cellulose carbamation can take place in either homogenous or heterogenous medium. The advantages of homogenous mediums are the even substitution of hydroxyl groups and better control of product characteristics. The cost of solvents is a disadvantage. (Heinze et al., 2018) A completely homogenous reaction environment is difficult to create, but has been done at least with deep eutectic solvents.

In the case of a heterogeneous reaction medium, such as a slurry, the reaction is more dependent on activation and interactions between the media. Due to this complexity, the typical reactions of organic chemistry are not easily transferable into cellulose chemistry. (Klemm et al., 2005) Most cellulose carbamation reactions are heterogenous, either in slurry form or between solid cellulose and gaseous HNCO.

Heterogenous reactions in a slurry form most often involve an inert solvent for urea, whereas the cellulose does not dissolve or dissolves only towards the end. These inert organic solvents include for instance xylene and N-methyl-2-pyrrolidone.

Supercritical CO_2, along with ethanol, has been utilized in impregnation at a high pressure in an autoclave. After the CO_2 treatment, the pressure was released and the carbamation was performed at 132,7 C for 3 hours. (Yin & Shen, 2007) Another supercritical CO_2-assisted carbamation was performed by placing urea, cellulose and ethanol separately into the autoclave, which was heated to 150-170 °C. The supercritical CO_2 was added and the reaction ran for 2-10 hours. (Zhang et al., 2013)

The vast majority of carbamation reactions get their heat from conventional heating, accompanied by long reaction times. To overcome them, microwaves have been utilized as a green and solvent-free method. The reaction times were in the scale of minutes. However, methods such as microwave and supercritical CO_2 require special equipment and are

extremely difficult and expensive to scale up. Another method with a short reaction time is the hot press at temperatures up to 220 °C (Vo et al., 2014). Hot presses are common in for example the textile, film and plywood industries.

Table 2. Overview of cellulose carbamation methods found in literature.

Method/Solvent	Impregnation	Reaction	Reference
Supercritical CO_2-assisted impregnation	Ethanol, supercritical CO2 and urea at 12-22 MPa and 40-50 °C	132,7 °C for over 3 h	Zhang et al., 2013; Yin & Shen, 2007
Carbacell	Xylene, urea and NaOH	Temperature 120-180 °C	German patent DE10253672B3; Fink et al., 2014
Liquid ammonia	Liquid ammonia and urea either in pressure vessel or -33 ° C	Temperature of 110-150 °C	Finnish patent FI62318C
Deep eutectic solvents (DES)	Urea-based DES and cellulose stirred at constant temperature for 20 h in 95-120 °C	Simultaneously with impregnation	Willberg-Keyriläinen et al., 2018
Microwave	30 % urea solution	Microwave at 255 W for 2-5 min	Guo et al., 2010
Microwave	0,9-4,5 % urea solution	Microwave at 380 W for 10-30 min	Gan et al., 2014
N-methyl-2-pyrrolidone (NMP)	NaOH solution	Urea and NMP, 135-165 ° C for 5-20 h	Xiong et al., 2017
N, N-dimethylacetamide (DMAc)	-	130-160 °C for 1-6 h	Yu et al., 2017
PEG 2000, LiCl, urea	PEG 2000, LiCl, urea	Hot press: pressure 1 bar, temperatures 150-220 °C, time 30s to 2min	Vo et al., 2010

5.3.1 Catalysts

Catalysts are substances that enable reactions to proceed at faster rates but don't take part in the reaction itself. Some catalysts have been utilized in different carbamation experiments. Vo et al. (2010) utilized sodium acetate which had a catalytic effect on carbamation with a hot press. Moreover, they elaborated that alkali metal salts in general have a catalytic effect on reactions between isocyanates and hydroxyl groups.

5.4 Washing

In many cases, cellulose carbamate is washed with water to remove impurities. This is done to avoid their accumulation in further processing stages and chemical recycling loops. In most cases the impurities are unreacted urea and nitrogenous by-products. Urea has an extremely high water solubility of up to 544 g/L at 25 °C. Biuret is the main nitrogenous by-product and has a water solubility of 15 g/L at 15 °C. (Yalkowsky et al., 2010) Considering that the amount of biuret is small, washing does not seem to take considerable efforts. If a minimal amount of urea is utilized, washing can even be abandoned completely (Fu et al., 2015).

Sample washing is particularly important before nitrogen content analysis to accurately determine DS, since nitrogenous by-products and unreacted urea can give a falsely high result. On the other hand, nitrogen content analyses can be useful in determining the extent of washing that is necessary to purify the sample.

6 Dissolution of cellulose and its derivatives in cold alkali

Cellulose dissolution is an important prerequisite for many applications, including for example characterization, homogenous syntheses and shaping into products such as fibers (Heinze et al., 2018). Regardless of the solution, the key to cellulose dissolution is the breakage of hydrogen bonds between the molecules, as well as overcoming hydrophobic interactions.

6.1 General aspects

Cellulose dissolution consists of several stages including solvent diffusion, swelling, decrystallization, chain disentanglement and diffusion into the bulk solution. (Shabbir, 2023) These stages are presented in figure 13. At first, when placed in contact with a solvent, the solvent molecules start permeating and diffusing into the cellulose structure, affecting both the crystalline and amorphous regions. At this stage, the solvent-cellulose interactions overcome the molecular forces between cellulose chains. Thus, the crystalline structures are broken down and the chains conformational movement increases. (Shabbir, 2023) This stage is also characterized by cellulose swelling, where the solvent permeates the cellulose structure, forming a heterogeneous swollen gel-like structure. The process may stop at the swelling stage if the polymer-solvent interactions are not strong enough. (Wertz et al., 2010) If they are, the second stage in dissolution becomes effective, and cellulose molecules start to disentangle from each other and diffuse into the bulk solution until completely separated. (Shabbir, 2023)

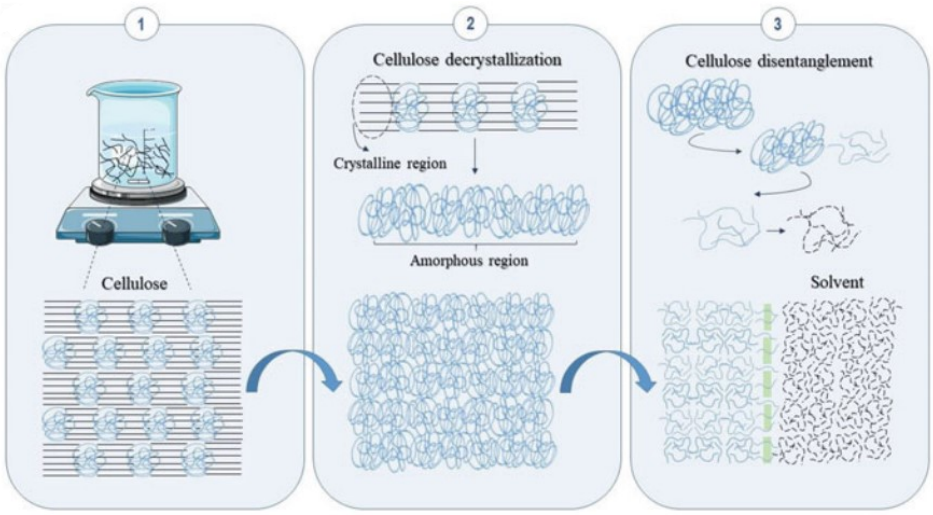

Figure 13. A schematic representation of cellulose dissolution: 1. Under stirring, the solvent diffuses into the cellulose structures with crystalline (black) and amorphous (blue) regions. 2. Cellulose decrystallizes, leaving the amorphous regions. 3. Cellulose molecule chains disentangle from each other and move into the bulk solution, where a dissolved equilibrium state is achieved. (Shabbir, 2023).

Alkali hydroxide solutions, including NaOH, cause strong swelling of cellulose, and also dissolution under a limited range of conditions. The swelling and dissolution are affected by

the NaOH concentration and temperature, as well as the cellulose structure, reactivity and the DP. (Heinze et al., 2018). Typically the solvent NaOH concentration is between 7-10 % and the temperature is between -5 to 1 degrees Celsius. (Budtova & Navard, 2016)

Additives like urea, thiourea and some metal oxides have been shown to improve cellulose dissolution when added to the solvent. ZnO is the most common metal oxide, typically added at a concentration of up to 2 % to improve the dissolution and stability of the solution. Urea has also been proven to improve dissolution of cellulose in concentrations of roughly 2-12 %. (Budtova & Navard, 2016) Therefore, residual urea in cellulose carbamate is not a concern for dissolution and can actually be beneficial. The downside of additives is their requirements for chemical recovery systems (Olsson & Westman, 2013).

Over time, cellulose-NaOH-water solutions lose their stability and transform irreversibly from a viscous liquid to a gel, *i.e.* a three-dimensional solid-like network. Gelation is caused by crosslinking between polymer chains or cellulose aggregates. A gel is an elastic, rubber-like solid that does not demonstrate any flow when its container is tilted. (Mulder, 2000) Therefore it is not processable into products such as fibers. Gelation is affected by at least the storage temperature, cellulose concentration and additives (Guo et al., 2011). Both ZnO and urea have been shown to delay gelation.

6.2 Carbamate dissolution in NaOH

Cellulose carbamation is known to improve its dissolution by weakening the hydrogen bonding network that facilitates the insolubility of cellulose. The effects of DS on CC dissolution in aqueous NaOH has been studied from various points of view.

According to Harlin (2019), the solubility of cellulose carbamate increased as its nitrogen content increased from 0 to 1.57 %, and subsequently decreased. Thus, an optimal N-content seems to be at around 1.5 %. However, differing numbers have been presented in literature, for example by Fink et al. (2014), whose N-content was as high as 2.5-4.5 %. One reason for this difference could be the use of ZnO, which Fink et al. (2014) did not mention in their article. Fu et al. (2015) found that the minimum nitrogen content required for solubility decreased from 2 % to 0.5 % when adding a small amount of ZnO. The addition of ZnO is

therefore not only significantly profitable for the stability of the solution but also for dissolution of lower substituted CCs.

Guo et al. (2011) studied the gelation behavior of CCs with different nitrogen contents, and found that higher nitrogen content solutions gelate more easily due to the carbamate groups promoting the formation of a cross-linking network and aggregates. The evenness and the pattern of substitution are also important factors in gelation - unevenly substituted cellulose chains cross-link and aggregate more easily (Sun et al., 2009).

II. Experimental part

7 Structure and objective of the experimental part

The objective of the experimental part stemmed from the interest to study different ways to perform the cellulose carbamation reaction. The methods were be chosen and reviewed according to their scalability and applicability to a pulp mill-integrated facility. Based on the findings of the literature part, the simplest and most scalable methods utilize urea and high temperatures to perform the reaction. Since the main reactant HNCO is a gas, the most attention was directed towards methods that have a closed or semi-closed environment during the reaction.

The first studied method was the hot press, which has the advantage of a short reaction time. The downside is that wet or moist materials can create a steam explosion and thus can't be utilized. Therefore, the time, temperature, urea dose and pulp properties were identified as the main factors that could affect the reaction. In addition, the short reaction time could possibly produce a less discolored product.

The second studied method was the closed reactor. The hypothesis was that the closed environment could increase the reaction efficiency. This method was also utilized to compare never-dried and dried pulp, with the hypothesis that never-dried pulp would have the advantage of better accessibility and thus extent of the reaction. In addition, some preliminary catalyst screening was done.

Both the closed reactor and the hot press method were compared to carbamation in a ventilated oven. The oven method is convenient for lab-scale, but it is not very scalable at least up to full scale. The oven also represents an open reaction environment, where the risk of losing evaporated urea and HNCO is evident.

Another objective of the experimental part was to characterize the CC products with suitable methods. An important target was to compare the elemental analysis and FTIR-ATR methods in determining degree of substitution. Quantitative FTIR-ATR is a fast and non-destructive measurement. In addition, the CED viscosities and CIELAB color coordinates were analyzed and measured to determine the DP and color, respectively, of the cellulose carbamates.

8 Materials and methods

8.1 Materials

The pulp obtained for carbamation was softwood Kraft pulp from UPM Kaukas mill. The different pulps and their pretreatments are presented in table 3.

Table 3. Different pulp materials utilized in carbamation experiments: their symbols and pretreatments.

Symbol	Stage of drying	Pretreatment	Experiments
A	Dried	None	Closed reactor
B	Never-dried	None	Closed reactor
C	Dried	Yes	Hot press, oven, preliminary tests

Urea was obtained from two different sources: purity >95 % was obtained from VWR and purity 99-100.5% was obtained from Sigma-Aldrich. Zinc chloride, zinc sulphate heptaydrate and sodium acetate were obtained as analytical grade.

The water utilized in all steps was reverse osmosis (RO) filtrated water.

8.2 Methods

The studied carbamation environments were oven, hot press and closed reactor. The pulps were impregnated with urea either with the sheet method or the disintegration method. All DMCs were analyzed according to the ISO 638-1:2022 standard.

8.2.1 Impregnation

Impregnation of sheets

The sheets were impregnated in 4 or 8% aqueous urea solution for 30 seconds and pressed through a rolling press with two rotating cylinders to remove excess urea solution. The sheets were dried horizontally in an oven at a temperature of 60 °C overnight. Some of the sheets were weighed prior to impregnation as well as after the wet pressing, and the urea dose per dry cellulose was calculated with equation 3.

$$w_{urea} = 100 * \frac{\frac{c}{100} * \frac{p_{urea}}{100} * \left(m_{wet} - m_{dry} * DMC\right)}{m_{dry} * DMC} \quad (3)$$

where

w_{urea}	urea mass per absolute dry cellulose, [%]
c	mass fraction of urea in impregnation solution, [%]
p_{urea}	purity of urea, [%]
m_{wet}	mass of the sheet after impregnation, [g]
m_{dry}	mass of the sheet before impregnation, [g]
DMC	dry matter content of the sheet before impregnation, [%]

Impregnation by disintegration

For never dried vs dried testing, pulp sheets were torn to small pieces and soaked in water overnight at room temperature. Never-dried pulp was thickened to obtain a homogenous starting material, which had the dry matter content of 18.6 %.

30g of absolute dry pulp was placed 2 L of water, and the suspension was disintegrated in a L&W disintegrator for 10 000 revolutions. The obtained suspension was squeezed manually and placed in a centrifuge. The obtained pulp cake was placed in a kneader-type mixer, and urea and the possible catalyst was added dry. The mixture was homogenized in a kneader for 10 minutes, and a homogenous, crumbly material with a dry matter content of approximately 35 % was obtained. The mixture was dried in an oven at 105 °C for varying times to obtain higher dry matter contents.

$$w_{urea} = \frac{m_{urea} * \frac{p_{urea}}{100}}{m_{pulp} * DMC}$$

Where m_{urea} mass of dry urea, [g]

m_{pulp} mass of pulp, [g]

8.2.2 Carbamation

Hot press

The impregnated, dried sheets were pressed with a Bürkle hot press machine for 1-3 min. The temperature of the press plates was 140-190 °C and the pressure was set to approximately 20 N/cm^2. This quite low level of pressure was chosen so that the sheet would not be compressed. The press was operated in a "fast closing" mode, where the pressure between plates overshot for around 15 seconds as they closed, and the timing started automatically as the pressure lowered to the set value. The sheets were folded twice to fit them inside the press. Two additional pieces of pulp sheet were placed under and on top of the carbamation sheet to protect it from impurities in the press plates. The temperature of the reaction was measured with a thermocouple which was inserted in the middle of the folded sheets, and coupled to a multimeter device displaying the temperature.

For the hot press experiment plan, a 2^3 factorial design was implemented according to table 4.

Table 4. Experimental design for the hot press experiments.

Name of experiment	**Temperature of the plates, [°C]**	**Pressing time, [min]**	**Urea concentration in impregnation, [%]**
HP1	190	1	4
HP2	170	1	4
HP3	190	3	4
HP4	170	3	4
HP5	190	1	8
HP6	170	1	8
HP7	190	3	8
HP8	170	3	8

Oven

The oven carbamation was performed at a ventilated oven at 150 ˚C for 2 h. To create a closed environment in the oven, the pulp sheet was enclosed in a heat-resistant plastic bag. The bag was slightly open, making the environment in fact semi-closed.

Closed reactor

The closed reactor was an air-bath vessel with six closed sample chambers. The chambers were rotated in heated air to obtain heating and mixing during the reaction. The temperature of the chambers was measured from three chambers, of which one was used for control of

the heating. The heating time was 1 h and the reaction time 2 h in 150 ˚C. Each chamber contained 45 g of dry cellulose and different amounts of water, urea and catalyst. The catalyst dose was 10 mol-% of the urea.

8.2.3 Washing

General washing procedure

All water used in washing was RO water. The carbamated pulp was soaked in water overnight and disintegrated with an immersion blender for about 20 seconds. Each roughly 10-30 g of sample was disintegrated in 2 L of water and washed in a vacuum suction Buchner funnel with 5 L of water until the wash water was clear in appearance. The obtained CC cakes were dried in 60 °C overnight. An example of the appearance of the CC cake and its wash water in the beginning of washing is presented in figure 14.

Figure 14. An example of the appearance of the carbamated pulp (left) and the washing water (right).

Washing test

To confirm whether the washing was sufficient to remove nitrogenous compounds, an additional washing test was conducted. To account for both unreacted urea and nitrogenous by-products, two materials were chosen for this test: a hot press-carbamated sheet (8% urea

impregnated, 190 °C for 3 min) and a sheet which had been impregnated with 8% urea and dried as described in chapter 8.2.1.

Each 10 g of pulp was diluted into 4 % consistency and soaked overnight. The pulp was disintegrated with an immersion blender for about 20 seconds and filtrated with a vacuum suction Buchner funnel. The studied wash water amounts were 0, 0.5, 1, 2 and 5 L. A separate sample was prepared for each sampling point. The Flash nitrogen content of the pulps was analyzed.

8.3 Thermogravimetric analyses

Thermogravimetric analysis (TG) of urea and urea-catalyst-mixtures were conducted in a nitrogen atmosphere on the Netzsch TG209 F1 Libra device. The analysis measures the changes of weight when a sample is heated. The TG curves were recorded at 5 ˚C/min heating rate. In addition, to simulate carbamation in a constant temperature, urea was heated on a 20 ˚C/min heating rate up to a certain temperature, after which the sample was kept in that temperature.

8.4 Characterization of products

The intrinsic viscosity of the pulps in cupriethylenediamine was analyzed with the ViscoClock Plus analyzator according to ISO 5351:2010 standard. The relative viscosity of the cellulose-cupriethylenediamine (CED) solution correlates with the average DP of the cellulose. Higher DP cellulose has a higher CED viscosity.

The nitrogen content of the washed pulps was analyzed with the Flash 2000 analyzator according to ASTM D5291-16 standard. The nitrogen content results were used to calculate the degree of substitution according to equation 4 (Vo et al., 2010). DS indicates the average number of -OH groups in cellulose which are substituted by carbamate groups. Therefore maximum value for DS is 3 – the corresponding maximum N% according to the equation is approximately 14.4 %.

$$DS = \frac{162 * N\%}{100 * 14 - 43 * N\%} \quad (4)$$

where DS degree of substitution, [-], range 0-3

N% nitrogen content of the CC sample, [%], range 0-14.4%

The yield of the carbamation reaction was calculated according to equation 5. The yield is defined here as the result of the nitrogen content divided by the stoichiomerical nitrogen content of the CC.

$$Y = \frac{N\%}{w_{urea} * \frac{M_N}{M_{urea}}} \quad (5)$$

where Y yield of the reaction

N% nitrogen content of the product, [%]

w_{urea} urea dose per dry cellulose, [%]

M_N molecular weight of nitrogen = 14.01 g/mol

M_{urea} molecular weight of urea = 60.01 g/mol

The CIELAB color coordinates were analyzed with the SpectroEye color analyzer using the D50 illuminator. The main objective was to find out if the changes of color perception in the samples can be detected with this method, and possibly comparing the carbamation methods and finding correlations with DS or reaction conditions. The carbamated samples were compared to their starting materials by calculating the changes in color coordinates according to equations 6-9.

$$\Delta L^* = L^* - L_0^* \quad (6)$$

$$\Delta a^* = a^* - a_0^* \quad (7)$$

$$\Delta b^* = b^* - b_0^* \quad (8)$$

$$\Delta E = \sqrt{(L^* - L_0^*)^2 + (a^* - a_0^*)^2 + (b^* - b_0^*)^2} \quad (9)$$

8.4.1 FTIR-ATR

FTIR spectroscopy is based on interactions of infrared radiation with the sample. It allows indirect and non-destructive qualitative and quantitative analyses of various samples. It has proven to be a useful technique in analyzing the DS of different polymers (Fei et al., 2017), including promising results for cellulose carbamate.

When cellulose is carbamated, typically a new characteristic peak appears at about 1705-1725 $\frac{1}{cm}$. The peak is attributed to the carbonyl stretching of the C=O structure. Several articles have reported an approximately linear correlation between nitrogen content and absorbance peak height or area ratios in cellulose carbamate samples. The carbonyl peak height or area is compared to the reference peak at approximately 1604-1630 $\frac{1}{cm}$. (Chen & Huang, 2001; Nada et al., 2000; Nozawa & Higashide, 1981) This peak location has been attributed to the bending of water which has been absorbed into the cellulose (Fei et al., 2017).

In this work, the peak ratio is obtained by a simplified method - dividing the carbonyl stretching peak height by the reference peak height to find the best correlation with the nitrogen content of the sample. Fourier transform infrared attenuated total reflectance (FTIR-ATR) spectra of the washed and dried samples was measured with the Nicolet 6700 FTIR spectrometer on a Smart iTR W diamond crystal with 32 scans. The background spectrum was collected before each measurement, and each sample was measured twice to obtain an average spectrum result. If the final result was clearly an outlier, the procedure was repeated, making the amount of measurements 4. The spectrum baseline was corrected to minimize errors. The whole data handling procedure is presented in figure 15.

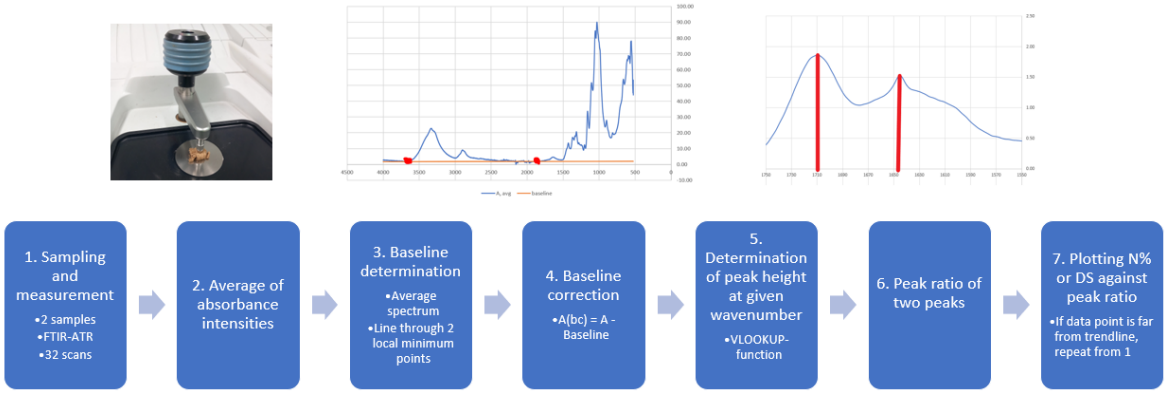

Figure 15. FTIR-ATR data acquisition and handling procedure to determine correlation between peak intensity ratios and degree of substitution for cellulose carbamate.

In addition, some samples were slightly pressed inside a screw bench pellet press. This was done to study the effect of sample pretreatment to the correlation.

8.5 Dissolution

The main goal of dissolution was to confirm that the cellulose carbamate could be dissolved sufficiently for further applications. In addition, the DS required for good solubility had to be determined to set minimum requirements for the synthesized CCs. This was done by dissolving samples which were involved in preliminary testing. The samples had varying nitrogen contents and preparation methods.

The cellulose carbamates were dissolved in 7.8 % aqueous NaOH and 1.3% ZnO solution. The temperature during dissolution was -6 - -5 ˚C . The solutions were kept in a refrigerator at a temperature of about 5 C. Their Brookfield viscosities were measured in this temperature according to SCAN-P 50:84 standard. In addition, to evaluate the solubility of the sample, the Kr filterability value was determined. Kr is dependent on the filtration rate, and is corrected by the viscosity of the solution. The analysis is performed by filtrating the cellulose solution and measuring the amount of filtered solution after certain times. (Eriksson et al., 2014)

9 Results and discussion

9.1 Thermogravimetric analyses

The TGA curve of urea at a 5 °C/min heating rate is presented in figure 16. The curve demonstrates that the mass loss of urea is quite slow in the temperature range of 130-200 °C. The formation of solid by-products in this temperature range can also be observed from the two-phase decomposition. The solid by-products are the residual mass at 260 °C and they are not fully decomposed until a temperature of about 350 °C.

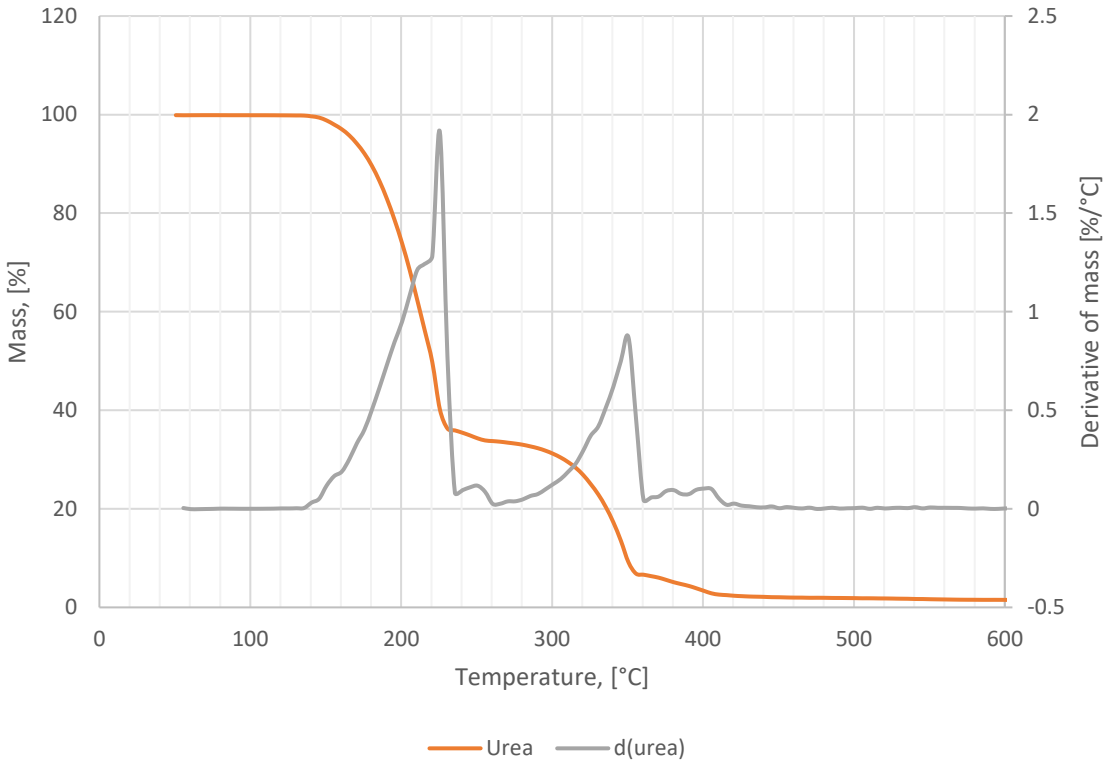

Figure 16. TGA curve of urea at the heating rate of 5 °C/min.

To obtain information about the behavior of urea in a constant temperature, three samples were analyzed by raising the temperature on a rate of 20 ˚C/min, and keeping the temperature constant for 45 minutes. The results are presented in figure 17. It can be concluded that the decomposition rate and the formation of residual solid by-products are accelerated by temperature. In addition, the decomposition of urea is quite a slow process and is preceded

by melting and evaporization. For this reason, a closed environment could be beneficial to keep the evaporated urea as well as the gaseous intermediates in the reaction environment.

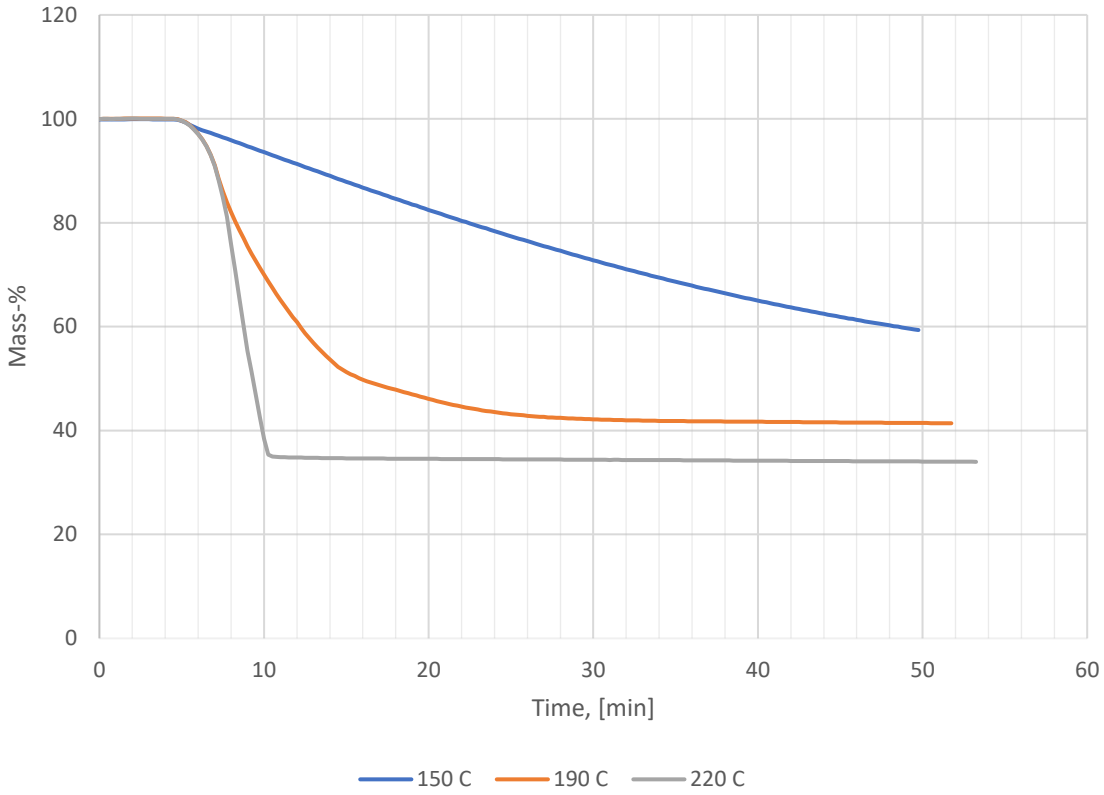

Figure 17. TG analyses of urea in three different constant temperatures: 150 ˚C, 190 ˚C and 220 ˚C.

9.2 Starting materials

The CED viscosities, Flash nitrogen contents and the dry matter contents were analysed and the results are presented in table 5.

Table 5. CED viscosities, nitrogen contents and dry matter contents of the starting material pulps.

Symbol	**CED viscosity, [mlg/g]**	**N_{pulp}, [%]**	**DMC, [%]**
A	751	0.03	95.9
B	850	0.03	18.6
C	188	0.01	92.0

Cellulose pulps can contain even up to 1% of “natural” or fixed nitrogen which is not washable (Goto et al., 2021). Whether the nitrogen contained in these starting material pulps is washable or not, was not investigated. Therefore, the nitrogen content of the starting materials will be considered only as a factor which might cause additional error in the results.

9.3 Preliminary testing and dissolutions

Some preliminary tests and dissolutions were conducted to assess the effect of different reaction conditions and nitrogen contents to dissolution. Pulp material C was chosen for its suitable CED viscosity. Some examples of the appearance of the CC solutions are presented in figure 18. The color differences originate from the color differences of the CCs.

Figure 18 Some examples of the appearance of the cellulose carbamate solutions. The solutions are arranged left-right from lowest nitrogen content to the highest.

The effect of CC nitrogen content on its Kr filterability index after dissolution is presented in figure 19. The samples with a nitrogen content lower than 0.2 % exhibit a quite linear decrease of the Kr filterability as the nitrogen content increases. The samples with a nitrogen content higher than 0.2 % exhibit Kr filterability values that are lower than 20. Despite the samples being prepared with different methods and urea doses, the Kr filterability values correlate quite well with the nitrogen content.

Based on figure 19, a minimum nitrogen content is 0.2 % for a successful cold alkali dissolution. However, since the pretreaments and their levels vary, it can not be generalized for all cases. More research is required outside the scope of this work to find the optimal nitrogen content for each case.

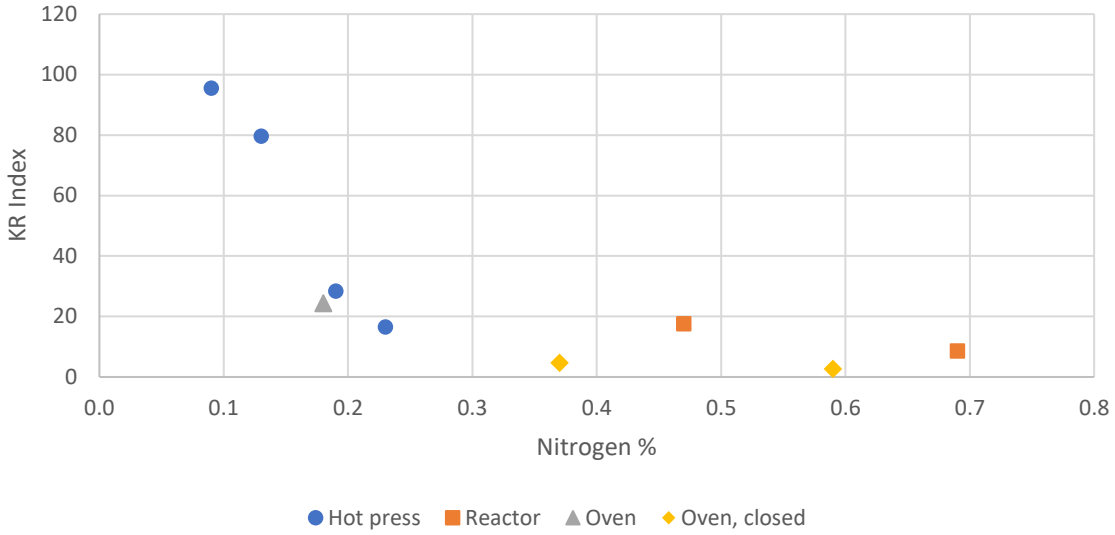

Figure 19. The effect of nitrogen content on the Kr filterability index of the CC solution.

In addition to pretreatment, the reaction environment can affect the CC properties and therefore its dissolution. In figure 19, the lowest Kr filterability values are obtained with the closed oven environment, even compared to the closed reactor. The reason for this is unclear, but the outcome is that a closed environment seems to be beneficial.

9.4 Hot press

9.4.1 Impregnations

The results of sheets impregnated with 4 % and 8 % urea solution are presented in table 6. The calculated average urea doses per dry cellulose were 3.3 and 6.8 % respectively. The sheets will be classified as 3 % and 7 % sheets from here on. The standard deviation is quite small, which implies that the sheet impregnation method is reproducible and precise.

Table 6. The results of the urea impregnations of sheets.

c = 4%			c = 8%		
m_{dry}, [g]	**m_{wet}, [g]**	**Urea dose, [%]**	**m_{dry}, [g]**	**m_{wet}, [g]**	**Urea dose, [%]**
508.6	869.5	3.26	505.9	878.7	6.74
503.1	862.2	3.28	504.7	882.5	6.84
507.9	868.1	3.26	511.6	885.3	6.69
509.4	872.6	3.27	513.0	886.6	6.67
513.3	876.2	3.25	500.5	878.9	6.90
	Average	3.26	512.6	880.5	6.59
	Standard deviation	0.01	504.0	880.0	6.82
				Average	6.75
				Standard deviation	0.11

9.4.2 Carbamations

The nitrogen contents of the hot pressed sheets are presented in figure 20, in respect to their final temperatures, *i.e.* the temperature right before the hot press opened. The trend of the nitrogen contents starts to increase after approximately 160 ˚C, which is in line with previous knowledge about urea decomposition - isocyanic acid is produced most effectively after 150 ˚C. Only the highest final temperatures reach over the goal of 0,2 %, indicating that the temperatures and times of under 190 ˚C and 3 min are not sufficient. No charring or carbonization of the sheets was observed, and therefore even higher temperatures and times could be beneficial.

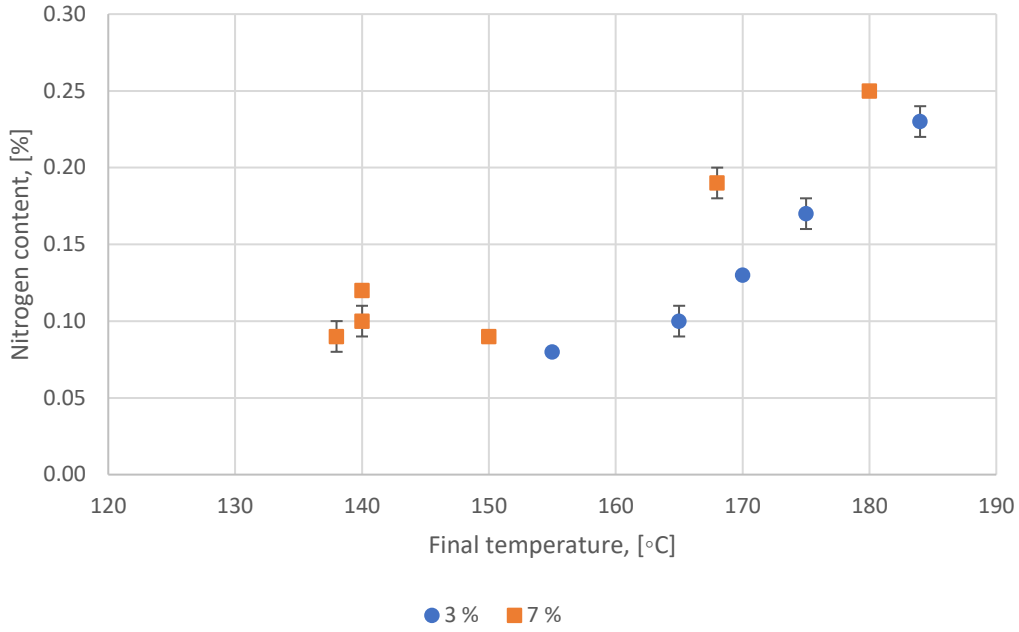

Figure 20. The nitrogen contents of hot press carbamated sheets plotted against the final temperature in hot pressing.

The yields of the hot press carbamations are presented in figure 21.

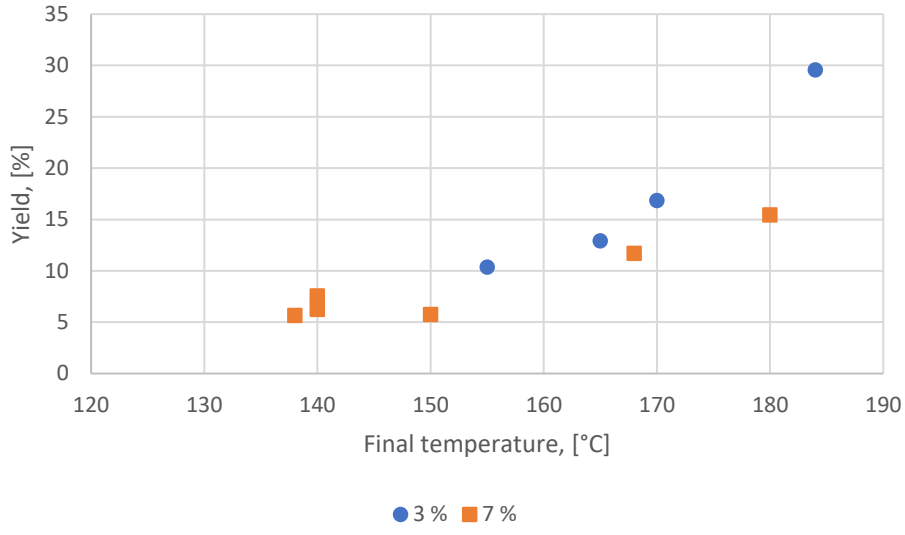

Figure 21. Yields of hot press carbamations plotted against the final temperatures.

The yields were higher for 3% urea especially at higher final temperatures. The highest yield (30 %) was obtained with 3% urea at 190 °C for 3 minutes. The respective nitrogen content was 0.23 %.

9.4.3 Analysis of effects

The main effects plot for nitrogen contents is presented in figure 22. It can be concluded that raising the levels of temperature, time and urea all increase the nitrogen content. The pressing time has the largest effect on the final nitrogen content, followed by temperature and urea dose.

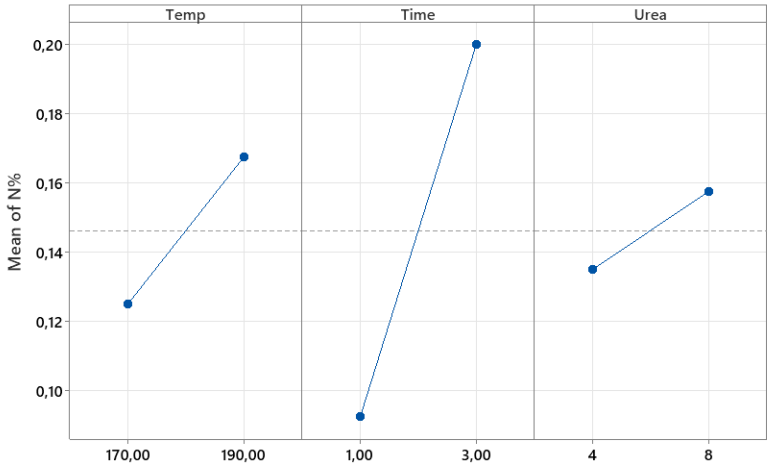

Figure 22. Main effects plot of fitted means for nitrogen content in hot press carbamations.

A simple regression model was created to help determine the effects and minimum conditions for a good quality product. To avoid overfitting, the interaction terms were left out. The regression equation in uncoded units is presented as equation 10. The coefficient term for time is the largest (0.0537), indicating that it has the largest effect. An R^2-value of 87.26% was obtained for the model, and the standard error was 0.03.

$$N\% = -0.378 + 0.00213 * Temp + 0.0537 * Time + 0.00563 * Urea \qquad (10)$$

The contour plots based on the regression model for the hot press carbamations are presented in figure 22. Contour plots help visualize the model which predicts the outcome of certain conditions. For example, the darkest shades of green in figure 23 represent the target nitrogen

content of over 0.20 %. The borders of these areas represent the minimal conditions which are required to achieve the value.

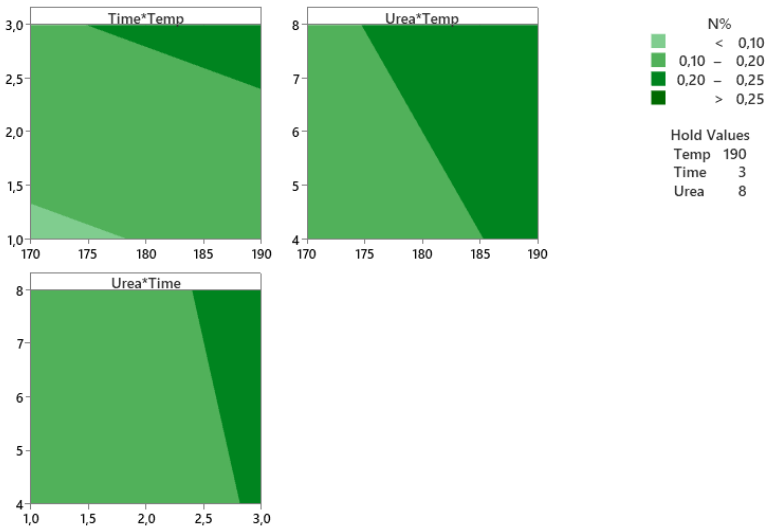

Figure 23. Contour plots for hot-press carbamation tests based on a regression model. The hold values represent the value of the third constant variable not depicted in each contour plot.

From the plots, some minimum values to achieve the target product can be estimated: time 2.5 min and temperature 175 ˚C. Above these values, the target is reached on all urea doses, but the minimum amount of urea still depends on the other factors.

9.5 Closed reactor

A closed air bath-heated reactor was used for comparison between never-dried and dried pulp, and catalyst testing for pulp A and B, as well as to study reaction conditions in general. The formation and accumulation of ammonia inside the reactor was clearly detected, as all the closed reactor samples had a strong smell of ammonia when taken out of the reactor. The smell was removed by washing.

9.5.1 Never dried versus dried

Pulps A and B were subjected to similar processing and conditions to see whether a difference in their reactivity can be noticed. The dry matter contents of the samples are presented in table 7.

Table 7. Drying times and dry matter contents for closed reactor samples in never-dried (ND) vs dried (D) testing.

Sample code	Drying time, [min]	DMC, [%]
ND1	105	88.9
ND2	30	42.9
ND3	0	36.2
ND4	105	86.2
ND5	30	45.2
ND6	0	37.8
D1	105	98.3
D2	70	83.1
D3	0	45.6
D4	105	95.9
D5	70	85.3
D6	0	47.4

It is evident that the lowest dry matter content, *i.e.* the samples which were only impregnated and centrifuged, was different for never-dried and dried pulps. For never-dried, it was approximately 35 % whereas for dried it was approximately 45 %. This is due to the hornification effect and reduced water retention ability in dried pulp. Because of this inherent difference in the pulp properties, the results which involve dry matter contents should not be interpreted as absolute. Instead, approximate extents of drying will be used in the data analysis part.

The nitrogen content results for never-dried and dried pulp are presented in figure 24A and B respectively. For never-dried pulp, nitrogen content of the products increases as dry matter content increases, ie more of the urea reacts as into CC. The increase is slightly steeper with 20 % urea dose than 4 % urea dose – therefore, increasing the urea dose has a bigger effect on the nitrogen content on high than low dry matter contents. This is all in line with the theory that water causes the isocyanic acid to decompose into ammonia and carbon dioxide. However, considering that the pulp was not pretreated, the nitrogen contents are high. The highest value was 0.34, which is even above the goal that was set for pretreated pulp in chapter 9.4.

In figure 24B, the most prominent result is the high nitrogen contents of the dried pulps at low urea dose – approximately twice as high as for never-dried pulp. The nitrogen content decrease with increasing dry matter content can be explained by a severe hornification effect, which is the consequence of thermal drying.

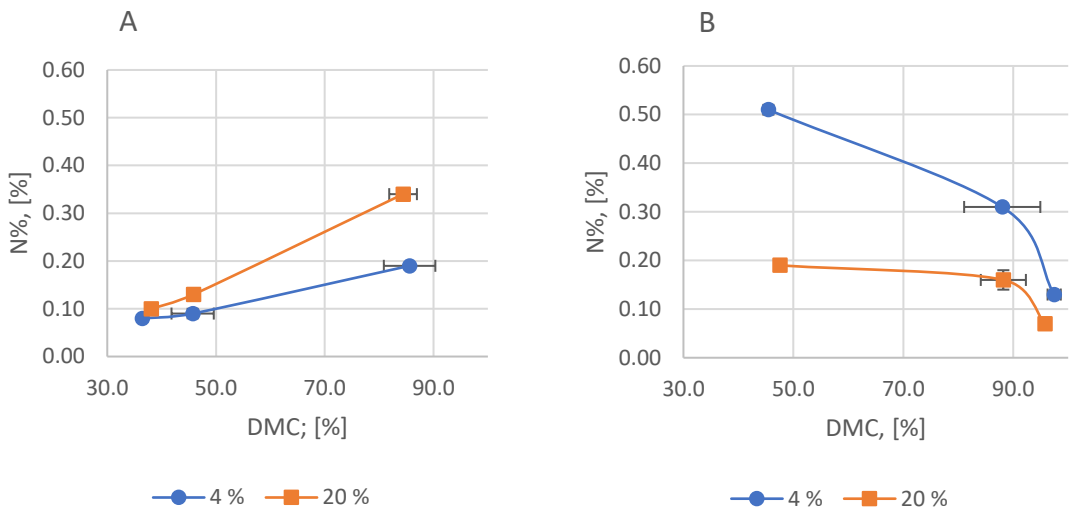

Figure 24. Air-bath carbamation nitrogen content results with differing dry matter contents for A) never-dried pulp and B) dried pulp.

The yields of the carbamation reactions for never-dried and dried pulps are presented in figure 25A and B respectively. The highest yields overall are obtained for 4% urea dose.

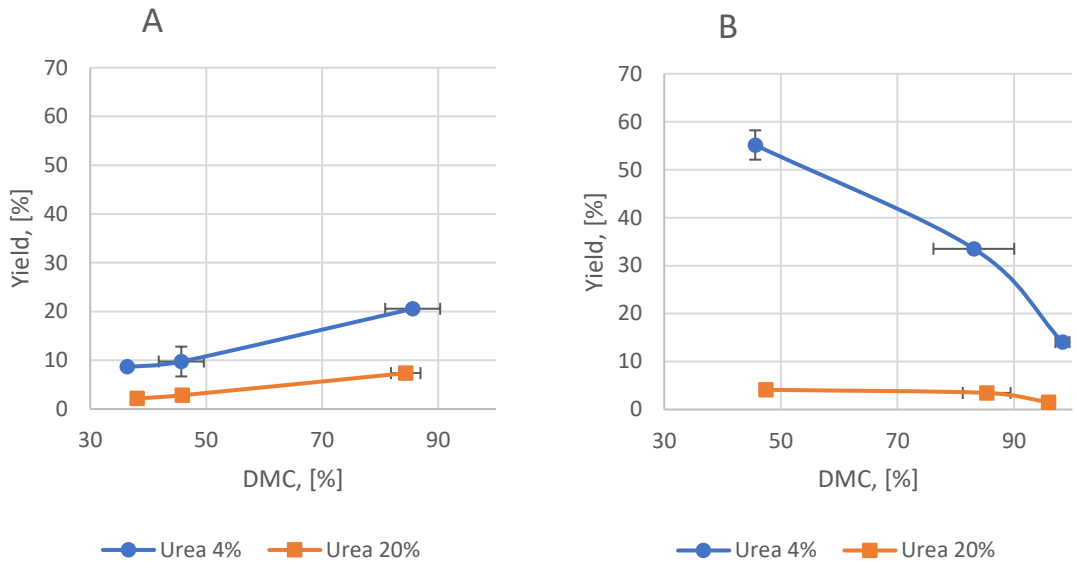

Figure 25. Air-bath carbamation yield results with differing dry matter contents for A) never-dried pulp and B) dried pulp.

The nitrogen contents of the closed reactor-carbamated pulps plotted against their CED viscosities are presented in figure 26A and B. It is evident that the CED viscosities of the samples have decreased to an unexpectedly low level. The decrease can be attributed to the autohydrolysis phenomenon, also called liquid hot water (LHW) treatment. Autohydrolysis begins at approximately 150 °C in the presence of pulp and water. The autohydrolysis process is catalyzed by the hydronium ions which are generated from water autoionization, as well as acetic acid generated from the decomposition of hemicellulose. The effect of acetic acid is much greater compared to the hydronium ions. These autocatalysts cause the hydrolysis of polysaccharides, *i.e.* cellulose. (Mussatto, 2016)

Comparing figures 24 and 26, it is evident that the CED viscosity has a higher effect on the extent of the reaction than the DMC. The effect is also the same for both dried and never-dried pulp – low CED viscosity leads to a higher nitrogen content. Therefore, this could be adopted as one possible explanation for the unexpectedly high nitrogen contents of certain samples.

In figure 26 B, the dried samples are spread along the x-axis (CED viscosity) on a range of approximately 270-600 ml/g. In contrast, the never-dried pulps in figure 25 A are not as spread on a narrower range of 290-360 ml/g. This could explain some of the drastic differences in the nitrogen content levels of never-dried and dried pulps. However, it does

not fully explain why the dried pulps obtained higher nitrogen contents in a similar environment and CED viscosity.

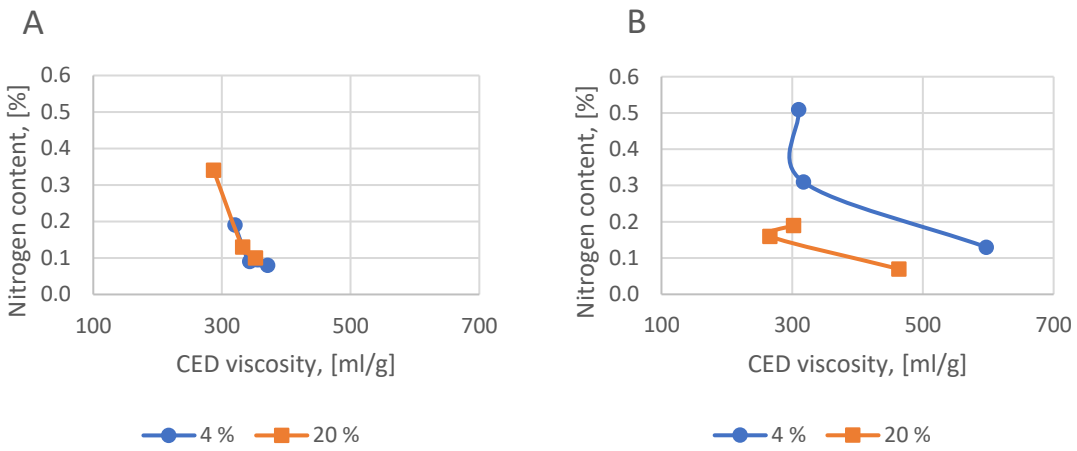

Figure 26. The nitrogen contents of closed reactor-carbamated pulps plotted against their CED viscosities. A) never-dried pulp, B) dried pulp.

All in all, the presence of an unexpected autohydrolysis reaction and its effect on the outcome made the analysis of data more complicated and somewhat inconclusive in the comparison of the dried and never-dried pulp. The results are not in line with general knowledge of differences between never-dried and dried pulp.

9.5.2 Catalyst screening

The appearances of the urea-catalyst mixtures for TG analyses are presented in figure 27. When the catalysts and urea were mixed, the formation of wet-appearing aggregates was observed for the zinc salts, whereas the appearance of the sodium acetate-urea mixture was a dry powder. This is caused by moisture absorption from air, which is a common occurrence with urea-zinc salt mixtures (Irfan et al., 2018).

Figure 27. Mixtures of urea and catalysts. Left: sodium acetate, center: zinc sulfate, right: zinc chloride.

The TG mass loss curves for the pure urea and catalyst samples are presented in figure 28. It can be observed that the samples with the Zn-salt catalysts decompose at a much slower rate compared to sodium acetate and pure urea. However, their mass loss starts earlier and ends later. Even at the end of the run at 900 degrees, not all urea-zinc chloride has decomposed. It is evident that the catalysts have an intrinsic effect on the behavior of urea. However, based on this data, it's difficult to predict the behavior of the different mixtures in the carbamation reaction.

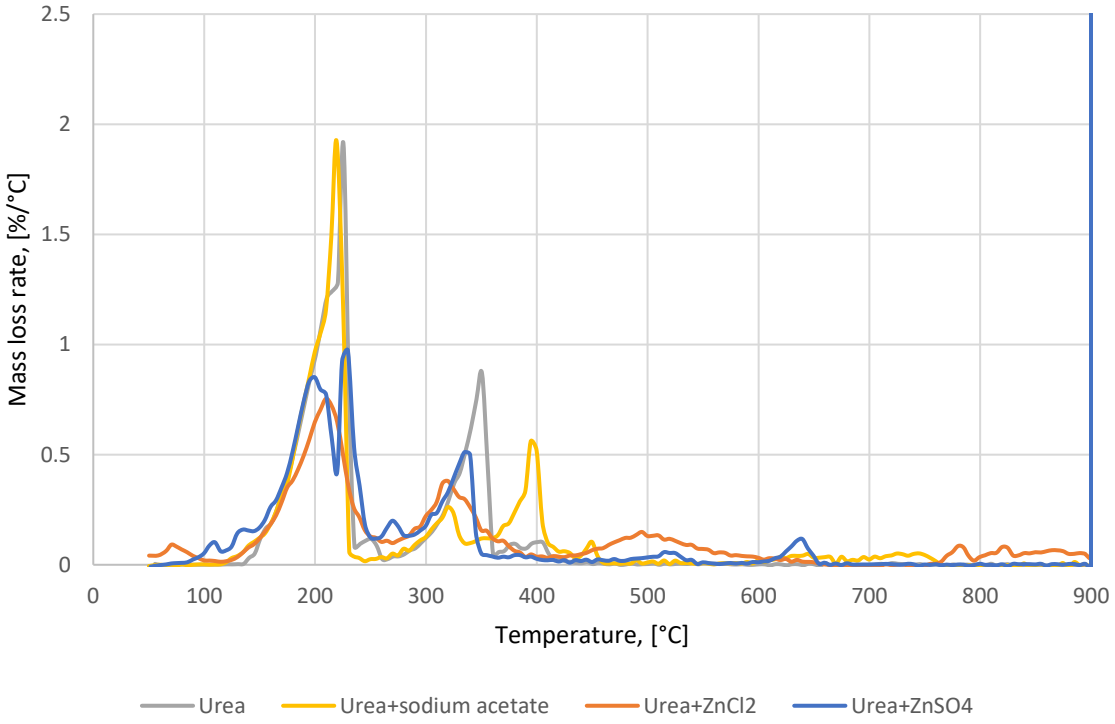

Figure 28. TG mass loss curves for pure urea and urea-catalyst mixtures.

9.5.3 Carbamation

The nitrogen content results of the different catalyst testing carbamations are presented in figure 29. On low DMCs, the nitrogen contents of all samples with a catalyst are on the same level or higher than the samples without catalyst. Therefore, it can be concluded that on low DMC levels, the presence of a catalyst does not have an effect on the carbamation.

On high DMC levels, the nitrogen contents of the samples with a catalyst are consistently only slightly higher than without catalyst. The only exception is sodium acetate at high DMC and high urea. Therefore it can be concluded that the catalyst has a positive effect on the carbamation reaction on high DMCs.

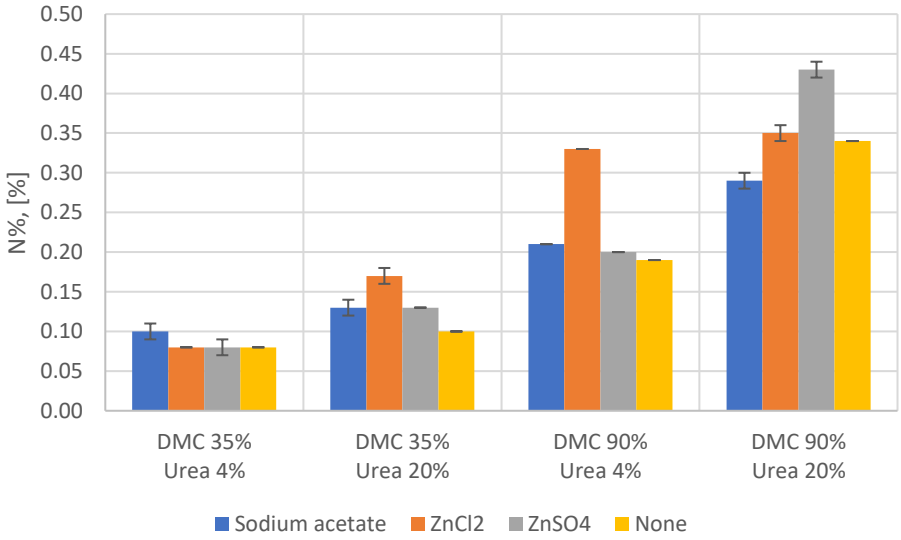

Figure 29. The nitrogen content results of catalyst screening tests on varying dry matter contents and urea doses. The error bars represent standard deviation.

The yields of the catalyst tests are presented in figure 30 A and B for 4 % and 20 % urea dose, respectively. Again, the yield is higher for the low urea dose. In all cases, high DMC results in a higher yield. As in previous results, there is again one result that lies significantly higher than the others in figure 30 A.

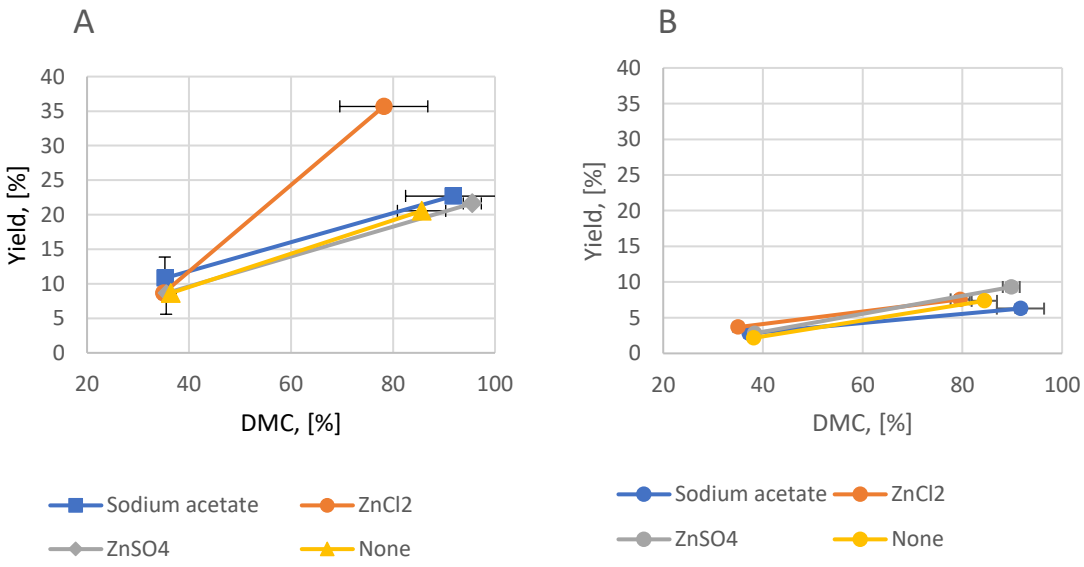

Figure 30. Cellulose carbamation yields obtained on different catalysts with A) Urea dose 4%, B) Urea dose 20%, in respect to the dry matter content during the reaction in a closed reactor.

The nitrogen contents of catalyst samples plotted against their CED viscosities are plotted in figure 31. As previously stated, it is evident that the autohydrolysis has a dominating effect

on the extent of the reaction. The highest nitrogen contents are obtained with the lowest CED viscosities of around 250 ml/g. As evident from figure 31, there was also one sample for which the autohydrolysis did not happen and the CED viscosity stayed over 700 ml/g. For this sample, the DMC was high (95.6%) which is a probable explanation to why the autohydrolysis did not happen.

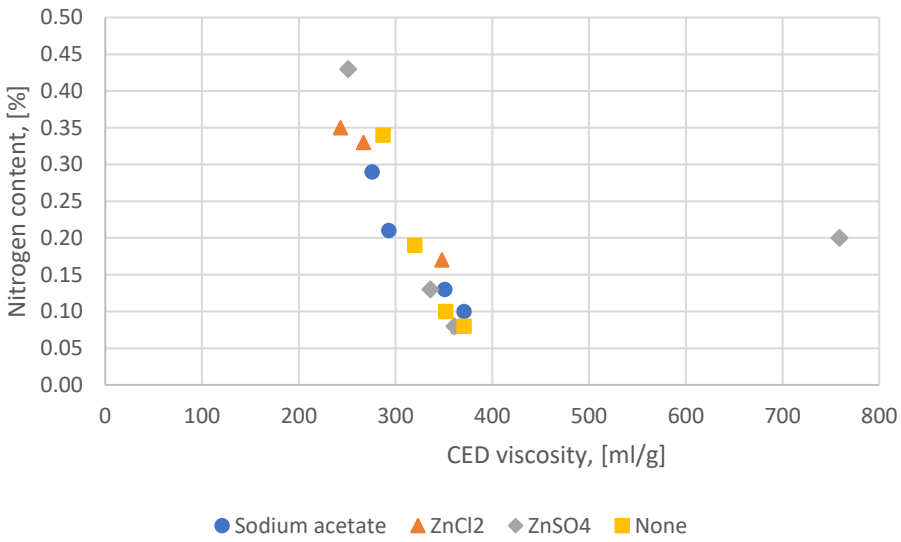

Figure 31. Nitrogen content results of catalyst screening CC samples plotted against their CED viscosities.

A main effects plot for the nitrogen content mean based on different factors is presented in figure 32. A main effects plot shows the mean effect from changing the levels of factors. For example, raising the urea dose from 4 % to 20 % raises the nitrogen content approximately 0.1 % on average.

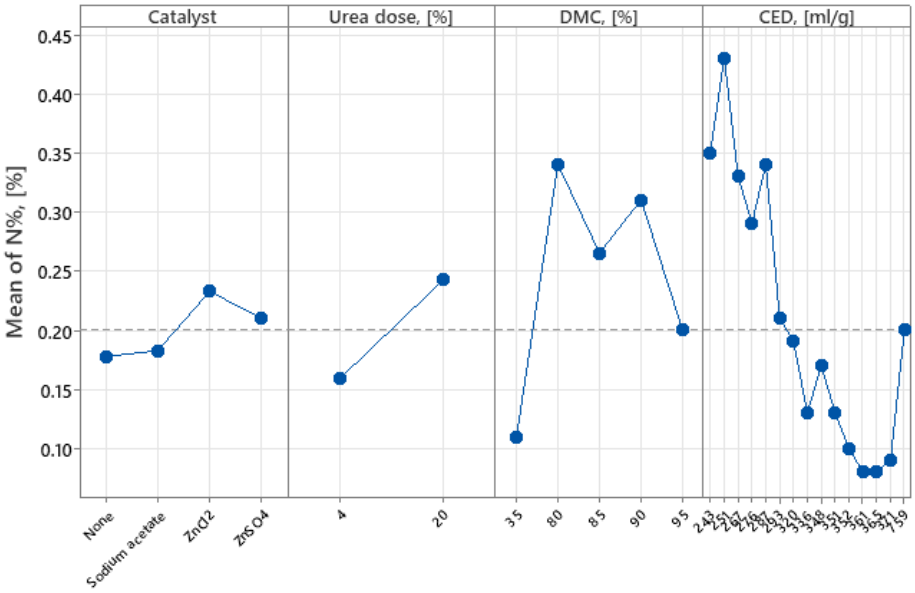

Figure 32. Main effects plots of catalyst screening samples.

When comparing the catalysts to the non-catalyst experiments, it is evident that the line between catalyst "None" and "Sodium acetate" is almost horizontal. This indicates that adding sodium acetate had no effect on the extent of the reaction. On the other hand, the addition of zinc salts had a positive effect – approximately 0.3 % for zinc sulphate and 0.5 % for zinc chloride. Therefore it can be concluded that zinc chloride was the best catalyst out of these options.

From figure 32 it can also be observed that the DMC and CED viscosity have the largeet effects on the nitrogen content. DMC seems to have the highest response at levels 80-90 %.

9.6 Oven carbamation

To accurately compare the ventilated oven and the reactor, two oven samples were prepared from never-dried pulp with the same pretreatments and 4 and 20% urea doses. The samples were not dried in an oven prior to carbamation, since they would dry in the oven anyway. The results of the oven samples are presented in table 8. The nitrogen content of the 4% sample is lower than all corresponding closed reactor samples. The nitrogen content of the 20% sample was on the same range as the corresponding reactor samples. The yield for both reference samples was approximately 10%, which indicates that this could be the maximum

yield for these conditions and materials. The CED viscosity dropped only very slightly, since no autohydrolysis took place.

Table 8. The dry matter contents, nitrogen contents, yields and CED viscosities for samples which were carbamated in a ventilated oven.

Urea dose, [%]	DMC, [%]	N%, [%]	Yield, [%]	CED viscosity, [ml/g]	Change in CED viscosity, [ml/g]
4	37.15	0.05	10.82	825	25
20	38.2	0.24	10.38	844	6

A comparison between carbamation of sheets in a ventilated oven, closed oven and hot press is presented in table 9. The sheets were pretreated and impregnated in the same way. The highest nitrogen content was obtained with the closed oven environment, followed by the hot press and ventilated oven. The CED viscosities of the samples were on a similar level. The lowest value, 146 ml/g was obtained with the closed oven method which indicates that the closed environment combined with the long reaction time induced some hydrolysis.

Table 9. A comparison of the oven carbamations in both open and closed environments and a selected hot press-carbamated sheet

	Urea dose, [%]	N%, [%]	CED viscosity, [ml/g]
Oven	3	0.18	158
Oven, closed	3	0.37	146
Hot press HP3	3	0.23	161

9.7 Washing test

The nitrogen contents of the washing test samples are presented in figure 32. The nitrogen contents of the samples before washing have quite large standard deviations, indicating that there were differences in the deposition of urea and/or by-products in the sheets. The result of the carbamated sheet is higher than the urea-impregnated sheet, which is not plausible.

The result variation falls inside the standard deviation, as depicted in figure 33, therefore this difference in probably caused by heterogeneity in the sample.

The nitrogen content of the pulp samples decreases rapidly until 0.5 L of washing water has been deployed. Between 0.5 L and 1 L of wash water deployment, no changes are observed. Between 1 L and 5 L wash water deployment, the results decrease slightly: by 0.2 % for the carbamated sheet and by 0.03 % for the urea-impregnated sheet.

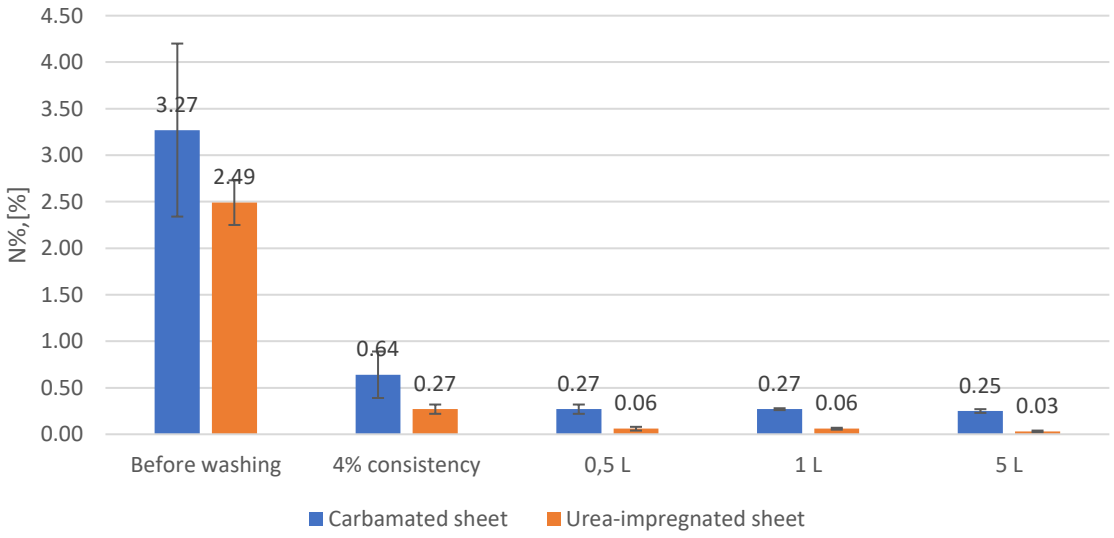

Figure 33. Nitrogen contents of the wash test pulp samples: carbamated sheet and urea-impregnated sheet.

Based on this data, it can be concluded that the dilution to 4% consistency and 5 L washing is well sufficient to remove nitrogenous products from the pulp for chemical analysis. The mass of washing water is more than 500 times the mass of the pulp washed, which is a large amount. It can be presumed that the 5 L of washing water is enough to remove all washable compounds entirely. In that case, dilution to 4 % consistency and washing by 0.5 L of water removes roughly 99% of the washable compounds, as can be seen in figure 34. This amount of water corresponds to a water:pulp ratio of 74:1.

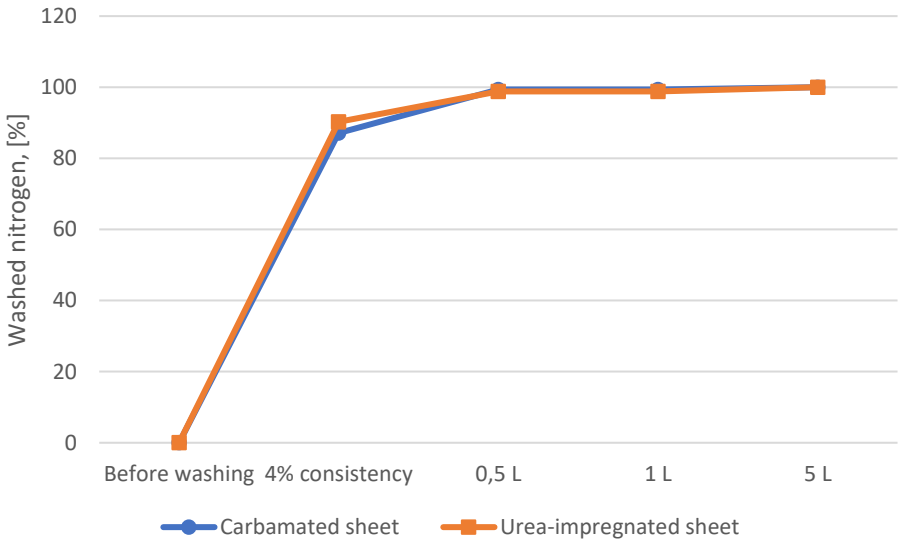

Figure 34. Percent of washed total nitrogen in the different stages of washing.

9.1 FTIR-ATR

The spectra of the starting material cellulose as well as some carbamated samples are presented in figure 35. As the degree of substitution increases, a small peak at approximately 1710 $\frac{1}{cm}$ appears next to the one at 1650 $\frac{1}{cm}$. The peak at 1710 $\frac{1}{cm}$ is attributed to the carbonyl (C=O) structure which is present in the carbamate group, and thus it confirms the formation of cellulose carbamate. Literature often reports also the decrease of the relative absorption peak at 3400 $\frac{1}{cm}$, which can not be seen clearly in this case, since the DS is too low. In fact, no other changes can be seen in the spectra as the DS increases.

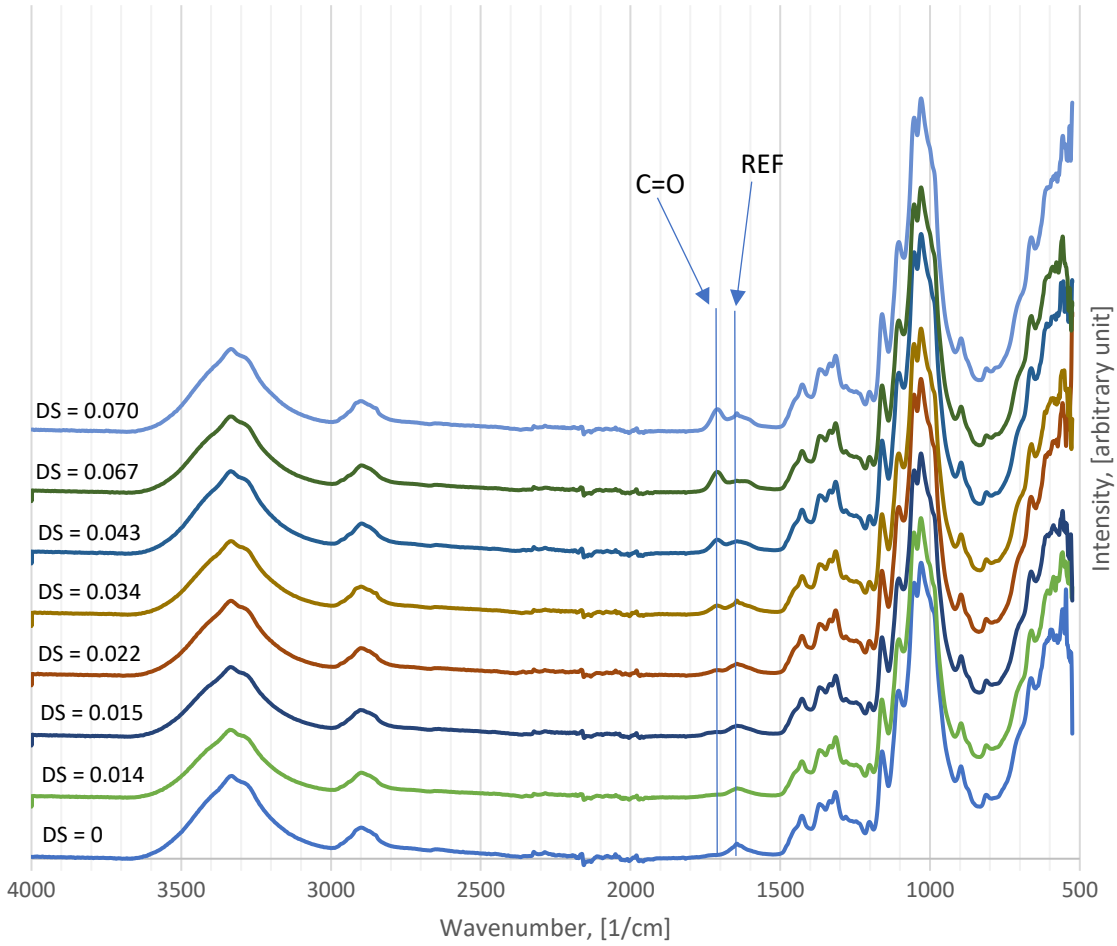

Figure 35. FTIR-ATR spectra of the starting material and selected carbamated celluloses with different degrees of substitution. The C=O and reference peaks are marked with lines and arrows.

The spectra of some samples indicated differences between overall peak intensities, as presented in figure 36. The peaks of DS=0.009 and DS=0.010 are substantially higher than the others samples. The intensities in an FTIR-ATR measurement increase as the contact between the sample and the crystal gets better, i.e. the air gaps are reduced, bringing more of the sample into the contact field of the crystal. The intensities tend to increase more rapidly at shorter wavelengths than longer ones. Therefore, when performing a quantitative analysis, it is beneficial to base the analysis on intensity ratios rather than single intensities. In addition, the error from sample contact can be minimized if the wavenumber range of the analysis is as narrow as is practical. (Perkin Elmer Inc, 2012)

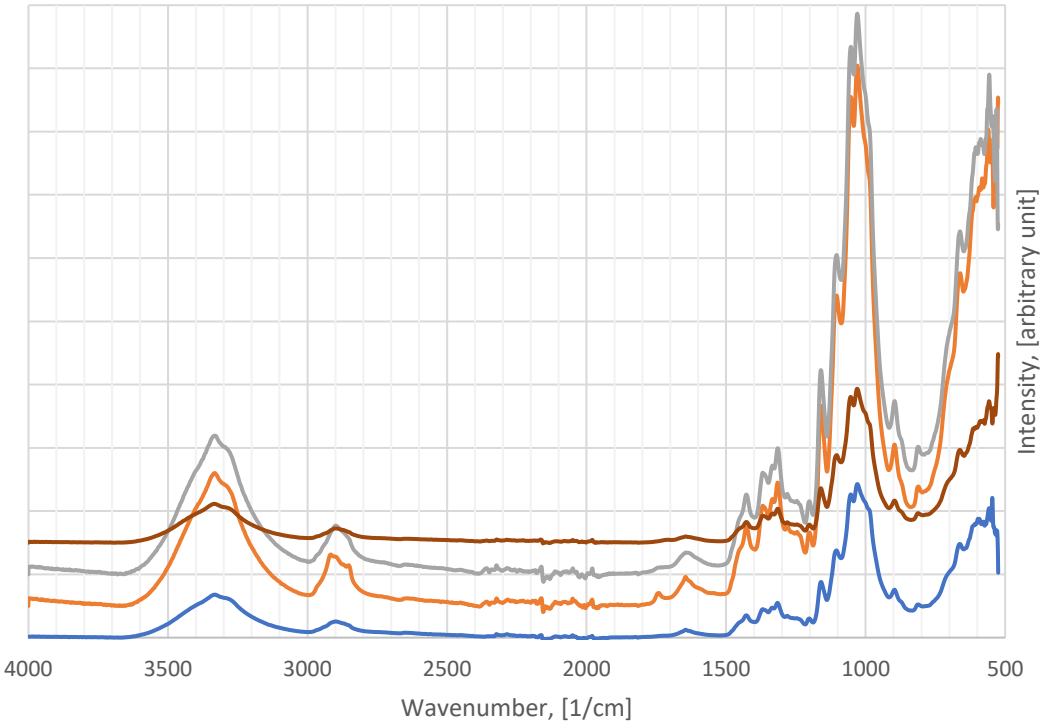

Figure 36. FTIR-ATR spectra of selected cellulose carbamate samples demonstrating different peak heights due to varying contact between the sample and the FTIR-ATR diamond.

To investigate whether the contact between the sample and the FTIR-ATR crystal could be improved with the available appliances, some samples were pressed. A comparison of the unpressed and pressed samples is presented in figure 37 A and B.

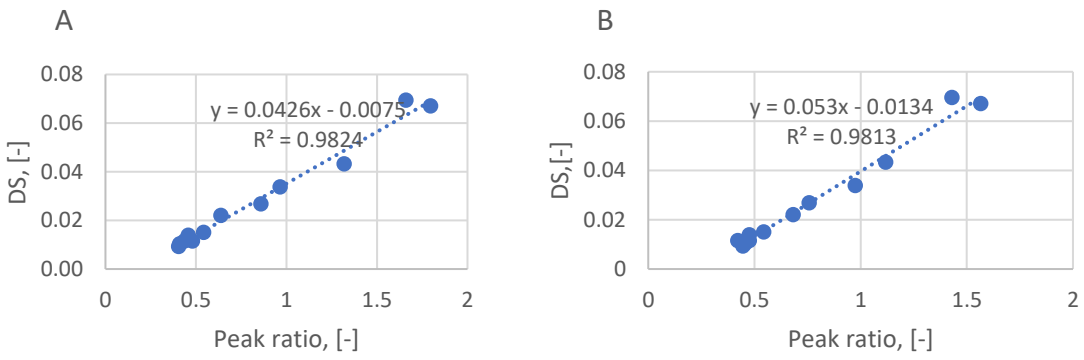

Figure 37. Comparison of the peak ratio-DS correlation between unpressed and pressed samples for FTIR-ATR: A) upressed, B) pressed.

It can be concluded from figure 37A and B that the pressing did not bring changes to the results. Peak ratios of the pressed samples were slightly higher, resulting in a steeper

trendline. The correlation between peak height ratio and DS was slightly worse for the pressed samples. Therefore, all other samples were only analysed unpressed.

The spectral data was analyzed regarding the correlations when plotting DS or N% versus peak ratio on varying peak ratios. Two peak ratios were chosen based in their highest correlations on linear trendlines: 1704 $\frac{1}{cm}$ / 1623 $\frac{1}{cm}$ which had the best correlation for overall data points, and 1709 $\frac{1}{cm}$ / 1625 $\frac{1}{cm}$ which had the best correlation for hot press and initial tests data points.

The linear correlation coefficients (R^2) are presented in table 10. The best values (approx.. 0.9) were found for samples which originated from hot press and initial tests. The closed reactor samples had considerably lower correlation compared to other samples. Baseline correction improved the correlation significantly for reactor samples and slightly for the other samples. In most cases, relating the nitrogen content instead of the DS to the peak ratio provided a slightly higher or similar correlation.

Table 10. Linear trendline R^2-values for selected peak ratios (horizontal axis = peak ratio). Comparison between baseline corrected and non-baseline corrected spectra, as well as vertical axis = N% and DS. The samples were divided to two categories: hot press+initial tests and closed reactor samples.

Peak ratio	1704 $\frac{1}{cm}$ / 1623 $\frac{1}{cm}$				1709 $\frac{1}{cm}$ / 1615 $\frac{1}{cm}$			
	Baseline corrected		**Not baseline corrected**		**Baseline corrected**		**Not baseline corrected**	
Vertical axis	**N%**	**DS**	**N%**	**DS**	**N%**	**DS**	**N%**	**DS**
Hot press + intial tests	0.974	0.974	0.923	0.921	0.983	0.982	0.933	0.931
Closed reactor	0.671	0.669	0.243	0.242	0.626	0.624	0.214	0.214
Overall	0.824	0.823	0.555	0.555	0.804	0.804	0.567	0.567

The best correlation (0.824) for all data points was obtained with baseline corrected peak ratio 1704 $\frac{1}{cm}$ / 1623 $\frac{1}{cm}$ and nitrogen content. The plot is presented in figure 38. It can be

observed that most of the outliers are closed reactor samples in the peak ratio region 0.8-1.0. The reason for this is unclear.

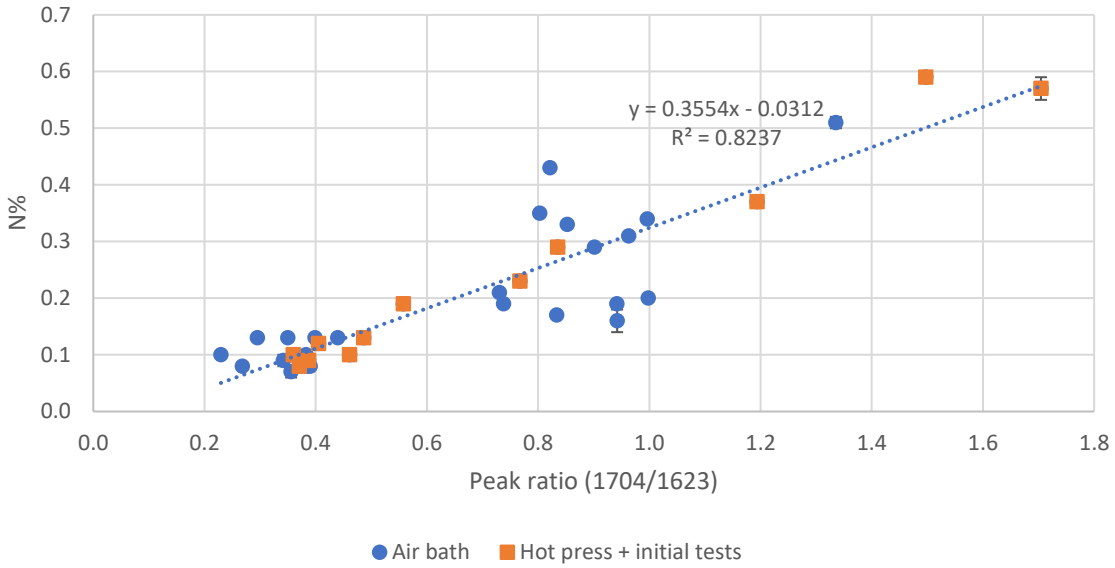

Figure 38. Nitrogen contents of carbamated pulps plotted against their FTIR-ATR peak ratios between peaks 1704 $\frac{1}{cm}$ and 1623 $\frac{1}{cm}$.

The standard error for the regression model, presented in appendix 3, was given as 0.061. At a 95% prediction interval, the error is 0.122. This error is quite high, and suggests that the used FTIR-ATR method would not be accurate enough to replace elemental analysis in the determination of N% and DS. However, most of the error occurred from closed reactor samples, indicating that the carbamation method has an effect. The utilized method was quite simplified, and possible further studies could include for example deconvolution to reduce the effect of peak overlap.

9.2 Color and whiteness of the samples

The color comparison of some unwashed and washed samples is presented in figure 39. The samples are much more yellow in color before washing – after washing, a white or medium brown color remains. This is probably caused by the removal of degraded carbohydrate and ammonia compounds from the wash water, since the water also removed the smell of ammonia. The samples prepared with the hot press or oven are significantly lighter, especially after washing, compared to the closed reactor samples.

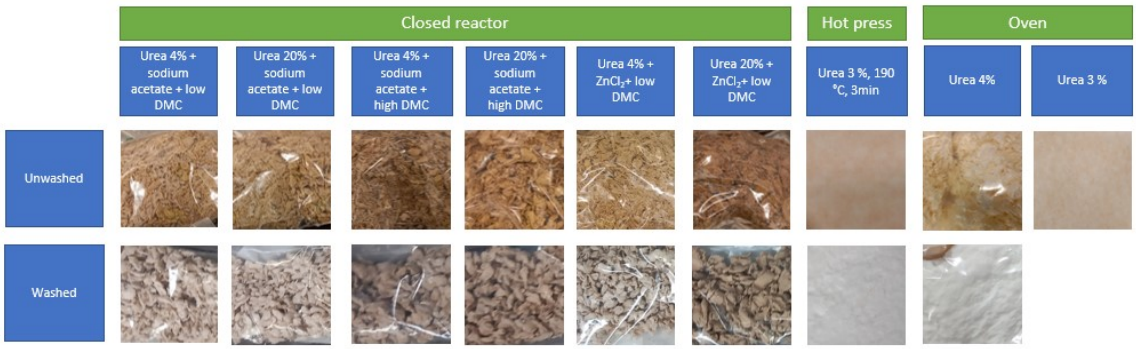

Figure 39. The appearances of some cellulose carbamate samples before and after washing.

From figure 39 it is evident that the closed reactor produced more discolored samples compared to the other methods. Comparing the unwashed oven and hot press samples, the color was nearly identical even though their heat treatment was significantly different. Therefore the discoloration should be attributed more to the carbamation itself than the duration of the heat treatment.

The CIELAB coordinates of some washed samples are presented in figure 40. It can be observed that the starting pulps B and C, along with some carbamated samples, are on an area closest to the (L*, a*, b*) white point (100,0,0). The carbamated samples are located on the positive axes of a* and b*, describing that they have yellowness and redness, respectively. Thus, carbamation discoloration can be attributed to decrease in brightness and increase in yellowness and redness which can be observed as decrease in L* and increase in a* and b*.

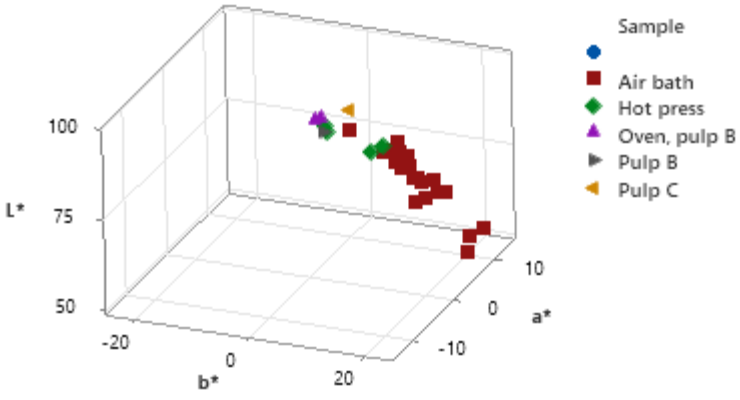

Figure 40. CIELAB color coordinates of the carbamated, washed cellulose samples presented as a three-dimensional scatterplot.

Main effects plots were plotted for the changes in coordinates between the closed reactor carbamated pulp and starting material. The plot for ΔE is presented in figure 41, and the plots for the individual coordinates are presented in appendix 2. Based on the plots, it can be concluded that the increase of reaction DMC caused a slight discoloration. Nitrogen content and decrease of CED viscosity (autohydrolysis) did not have an effect until high levels of 0.20 % and 500 ml/g respectively. At levels higher than these values, their discoloration effect was considerable. Catalyst samples were in general more discolored than non-catalyst samples. Out of the catalysts, zinc chloride produced the most discolored product.

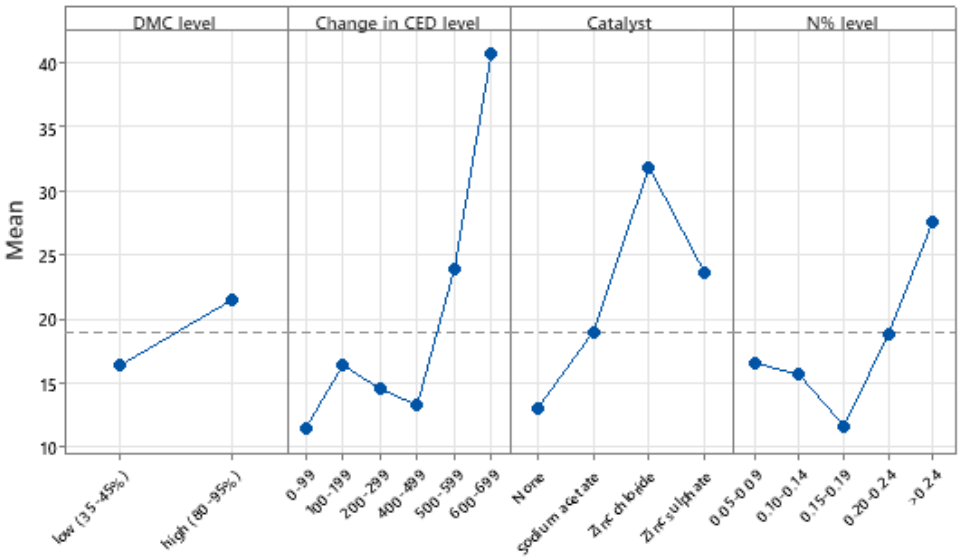

Figure 41. Main effects plot of the CIELAB color difference for pulps carbamated in different conditions and with different nitrogen contents. The carbamated pulps were compared to their starting materials to calculate the color difference.

Conclusions

Cellulose carbamate has recently gained attention as an emerging alternative to the viscose process for the production of environmentally friendly man-made cellulosic textile fibers. Cellulose carbamate has the advantage of good stability of the derivatized pulp, and therefore centralized production is possible. If the production facility is integrated to a pulp mill, savings can be made.

The objectives of this thesis originated from the desire to study different ways to perform the cellulose carbamation reaction. The scope was to compare a couple different methods and their reaction conditions and assess their scalability. The carbamation methods were chosen based on the hypothesis that a closed environment could be beneficial, since it prevents isocyanic acid, the reactant, from escaping. In addition, the presence of water inside the reaction environment was an interesting aspect, since drying is one of the most energy-intensive process steps. Catalysts have been reported to improve the reaction in some cases, and therefore the catalyst screening was done.

The hot press tests produced carbamated cellulose sheets which had the desired properties – first of all, the DS required for successful dissolution. In the beginning, it was determined that the minimum DS should be about 0.2 % to facilitate a good dissolution for this specific material. This is in fact quite low compared to literature, where the minimum nitrogen content typically varies from 0.5 - 4.5 %. The nitrogen contents obtained with the hot press were also low compared to those obtained by Vo et al. (2014). They obtained nitrogen contents of approximately 1.2 – 2.2 % - however, they utilized cellulose II fabrics and some higher temperatures as well as additives.

The minimum conditions for obtaining a nitrogen content of 0.2 % were determined to be approximately: temperature of the plates 175 °C and pressing time 2.5 minutes. The urea dose could possibly be lowered even below 3 %, since all urea doses achieved the goal at the highest temperatures and times.

The main shortcoming of hot press carbamation tests in terms of data analysis was that they were conducted on a quite narrow range of variables. Therefore, the overall conclusions are providing only some minimum conditions for an acceptable result. If the goal was to

maximize the result, all the variables should be maximized in the studied range. Increasing the ranges would have provided more information, and therefore more rounds are required to develop or fully optimize the process.

The closed reactor tests proved to be a powerful method for carbamation and hydrolysis of cellulose. Due to the high temperature, pressure and presence of water, an autohydrolysis reaction occurred. As a consequence, the DPs of the pulps decreased significantly, apart from the dryest sample with a dry matter content of over 95%. The autohydrolysis was not intentional and therefore it complicated the analysis of data. It was concluded that the autohydrolysis significantly promoted the carbamation reaction, even so much that the analysis of other factors became difficult. For instance, the comparison between never-dried and dried pulp should be treated as inconclusive and requires more experiments to obtain a reliable result.

The hydrolysis of cellulose is a beneficial process when considering cellulose dissolution and modification, since lower DP accounts for better reactivity and dissolution. Gan et al. (2017) studied autohydrolysis as a pretreatment process for NaOH/Urea dissolution and found out that autohydrolysis enhanced cellulose solubility and reduced the DP. However, autohydrolysis is a rapid and complex process (Mussatto, 2016), so the DP control might not be sufficient to meet the requirements of dissolution. Overall, the suitability of the described method should be further investigated from the dissolution point of view.

The catalysts – sodium acetate, zinc chloride and zinc sulphate – slightly improved the extent of the reaction. The biggest effect was observed on zinc chloride and zinc sulphate, indicating that zinc salts are an interesting topic for further research.

The color of the samples was monitored both visually and with a pulp whiteness indicator utilizing the CIELAB color coordinates. It was concluded that the discoloration was dependent on the extent of carbamation: oven and hot press samples produced similar discolorations despite different heating temperatures and times. The closed reactor samples were in general more discolored than the other methods. Their discoloration was mainly dependent on the extent of the autohydrolysis, DS and the utilized catalyst.

Washing the final cellulose carbamate free from nitrogenous by-products and unreacted urea is a crucial process for determining the DS of the product. The utilized wash water amount was large (more than 500 times the mass of pulp), but its sufficiency was still confirmed

with a simple washing test. It was concluded that washing with a water:pulp ratio of 74:1 was sufficient to remove 99 % of all removable nitrogenous compounds.

One additional objective of this thesis was to study whether the nitrogen content or DS of the carbamated celluloses could be analyzed by utilizing FTIR-ATR instead of elemental analysis. The correlation between the height of the C=O peak of the carbamate group and a reference peak showed good correlations with samples originating from hot press and initial testing. On the other hand, the correlations were much poorer for reactor samples. This indicates that the synthesis method has some profound effect on the properties of the cellulose carbamate and that one FTIR-ATR method can not be generalized for all of them. However, the data analysis methods used in this thesis for FTIR-ATR were simple and possibly the results could be improved by refining the methods. For example, peak areas could be utilized in calculations instead of peak heights.

References

Abushammala, H., & Mao, J. (2019). A review of the surface modification of cellulose and nanocellulose using aliphatic and aromatic mono- And di-isocyanates. In *Molecules* (Vol. 24, Issue 15). https://doi.org/10.3390/molecules24152782

Ahn, K., Zaccaron, S., Zwirchmayr, N. S., Hettegger, H., Hofinger, A., Bacher, M., Henniges, U., Hosoya, T., Potthast, A., & Rosenau, T. (2019). Yellowing and brightness reversion of celluloses: CO or COOH, who is the culprit? *Cellulose*, *26*(1). https://doi.org/10.1007/s10570-018-2200-x

American Chemical Society. (2021). *Urea*. https://www.acs.org/molecule-of-the-week/archive/u/urea.html

Borduas, N., Place, B., Wentworth, G. R., Abbatt, J. P. D., & Murphy, J. G. (2016). Solubility and reactivity of HNCO in water: Insights into HNCO's fate in the atmosphere. *Atmospheric Chemistry and Physics*, *16*(2). https://doi.org/10.5194/acp-16-703-2016

Budtova, T., & Navard, P. (2016). Cellulose in NaOH–water based solvents: a review. In *Cellulose* (Vol. 23, Issue 1). https://doi.org/10.1007/s10570-015-0779-8

Chen, G. M., & Huang, Y. P. (2001). Deconvolution Method for Determination of the Nitrogen Content in Cellulose Carbamates. *Chinese Chemical Letters*, *12*(4).

Ciolacu, D., & Popa, V. I. (2010). *Cellulose allomorphs: Structure, accessibility and reactivity*. https://www.researchgate.net/publication/257067594_Cellulose_allomorphs_Structure_accessibility_and_reactivity

Crnčević, D. S. (2018). *The Maillard reaction : an overview*.

Dubowik, M., Przybysz, P., Kucner, M., & Buzała, K. (2014). Influence of number of drying cycles on cellulose fibers hornification process. *Annals of Warsaw University of Life Sciences - SGGW. Forestry and Wood Technology*.

El Seoud, O. A., Kostag, M., Jedvert, K., & Malek, N. I. (2020). Cellulose Regeneration

and Chemical Recycling: Closing the “Cellulose Gap” Using Environmentally Benign Solvents. In *Macromolecular Materials and Engineering* (Vol. 305, Issue 4). https://doi.org/10.1002/mame.201900832

Eriksson, H., Wallenius, M., Ab, D. F., & Sundman, O. (2014). *Cellulose reactivity : difference between sulfite and PHK dissolving pulps*. https://urn.kb.se/resolve?urn=urn:nbn:se:umu:diva-93965

Ershova, O., da Costa, E. V., Fernandes, A. J. S., Domingues, M. R., Evtuguin, D. V., & Sixta, H. (2012). Effect of urea on cellulose degradation under conditions of alkaline pulping. *Cellulose*, *19*(6), 2195–2204. https://doi.org/10.1007/S10570-012-9791-4

Fei, P., Liao, L., Cheng, B., & Song, J. (2017). Quantitative analysis of cellulose acetate with a high degree of substitution by FTIR and its application. *Analytical Methods*, *9*(43), 6194–6201. https://doi.org/10.1039/C7AY02165H

Fink, H. P., Ganster, J., & Lehmann, A. (2014). Progress in cellulose shaping: 20 years industrial case studies at Fraunhofer IAP. *Cellulose*, *21*(1). https://doi.org/10.1007/s10570-013-0137-7

Fu, F., Xu, M., Wang, H., Wang, Y., Ge, H., & Zhou, J. (2015). Improved Synthesis of Cellulose Carbamates with Minimum Urea Based on an Easy Scale-up Method. *ACS Sustainable Chemistry and Engineering*, *3*(7). https://doi.org/10.1021/acssuschemeng.5b00219

Fu, F., Yang, Q., Zhou, J., Hu, H., Jia, B., & Zhang, L. (2014). Structure and properties of regenerated cellulose filaments prepared from cellulose carbamate-NaOH/ZnO aqueous solution. *ACS Sustainable Chemistry and Engineering*, *2*(11). https://doi.org/10.1021/sc500559g

Gan, S., Zakaria, S., Chen, R. S., Chia, C. H., Padzil, F. N. M., & Moosavi, S. (2017). Autohydrolysis processing as an alternative to enhance cellulose solubility and preparation of its regenerated bio-based materials. *Materials Chemistry and Physics*, *192*, 181–189. https://doi.org/10.1016/J.MATCHEMPHYS.2017.01.012

Gan, S., Zakaria, S., Chia, C. H., Kaco, H., & Padzil, F. N. M. (2014). Synthesis of kenaf cellulose carbamate using microwave irradiation for preparation of cellulose membrane. *Carbohydrate Polymers*, *106*(1).

https://doi.org/10.1016/j.carbpol.2014.01.076

Gerrard, J. (2005). The Maillard Reaction: Chemistry, Biochemistry and Implications by Harry Nursten. *Australian Journal of Chemistry*, *58*(10). https://doi.org/10.1071/ch0505_br

Goto, T., Zaccaron, S., Bacher, M., Hettegger, H., Potthast, A., & Rosenau, T. (2021). On nitrogen fixation and "residual nitrogen content" in cellulosic pulps. *Carbohydrate Polymers*, *253*, 117235. https://doi.org/10.1016/J.CARBPOL.2020.117235

Guo, Y., Zhou, J., Wang, Y., Zhang, L., & Lin, X. (2010). An efficient transformation of cellulose into cellulose carbamates assisted by microwave irradiation. *Cellulose*, *17*(6). https://doi.org/10.1007/s10570-010-9446-2

Guo, Y., Zhou, J., & Zhang, L. (2011). Dynamic viscoelastic properties of cellulose carbamate dissolved in naoh aqueous solution. *Biomacromolecules*, *12*(5). https://doi.org/10.1021/bm200331g

Harlin, A. (2019). Cellulose carbamate: production and applications. In *VTT Technical Research Centre of Finland*.

Heinze, T., El Seoud, O. A., & Koschella, A. (2018). *Cellulose Derivatives*. https://doi.org/10.1007/978-3-319-73168-1

Hill, J. W., & Jacobson, R. A. (1937). *Chemical process* (US2134825A). https://patents.google.com/patent/US2134825A/en

Iller, E., Stupińska, H., & Starostka, P. (2007). Properties of cellulose derivatives produced from radiation-Modified cellulose pulps. *Radiation Physics and Chemistry*, *76*(7). https://doi.org/10.1016/j.radphyschem.2006.12.002

Irfan, M., Khan Niazi, M. B., Hussain, A., Farooq, W., & Zia, M. H. (2018). Synthesis and characterization of zinc-coated urea fertilizer. *Journal of Plant Nutrition*, *41*(13). https://doi.org/10.1080/01904167.2018.1454957

Kantola, J., Råmark, H., Valta, K., & Vanhatalo, K. (2018). *Method for producing cellulose carbamate* (Fl 128164 B). https://patents.google.com/patent/FI128164B/en

Kee, J., Cardell, L., & Zereyesus, Y. A. (2023). *USDA ERS - Global Fertilizer Market Challenged by Russia's Invasion of Ukraine*. Amber Waves Magazine.

https://www.ers.usda.gov/amber-waves/2023/september/global-fertilizer-market-challenged-by-russia-s-invasion-of-ukraine/

Klemm, D., Heublein, B., Fink, H. P., & Bohn, A. (2005). Cellulose: Fascinating Biopolymer and Sustainable Raw Material. *Angewandte Chemie International Edition*, *44*(22), 3358–3393. https://doi.org/10.1002/ANIE.200460587

Kontturi, E. (2018). Supramolecular Aspects of Native Cellulose: Fringed-fibrillar Model, Leveling-off Degree of Polymerization and Production of Cellulose Nanocrystals. In *Cellulose Science and Technology*. https://doi.org/10.1002/9781119217619.ch12

Ly, B. C. K., Dyer, E. B., Feig, J. L., Chien, A. L., & Del Bino, S. (2020). Research Techniques Made Simple: Cutaneous Colorimetry: A Reliable Technique for Objective Skin Color Measurement. *Journal of Investigative Dermatology*, *140*(1), 3-12.e1. https://doi.org/10.1016/J.JID.2019.11.003

Mendes, I. S. F., Prates, A., & Evtuguin, D. V. (2021). Production of rayon fibres from cellulosic pulps: State of the art and current developments. *Carbohydrate Polymers*, *273*, 118466. https://doi.org/10.1016/J.CARBPOL.2021.118466

Mo, W., Chen, K., Yang, X., Kong, F., Liu, J., & Li, B. (2022). Elucidating the hornification mechanism of cellulosic fibers during the process of thermal drying. *Carbohydrate Polymers*, *289*, 119434. https://doi.org/10.1016/J.CARBPOL.2022.119434

Mulder, M. (2000). *Phase Inversion Membranes*. Encyclopedia of Separation Science. https://www.sciencedirect.com/referencework/9780122267703/encyclopedia-of-separation-science

Mussatto, S. I. (2016). *Biomass fractionation technologies for a lignocellulosic feedstock based biorefinery*.

Nada, A. A. M. A., Kamel, S., & El-Sakhawy, M. (2000). Thermal behaviour and infrared spectroscopy of cellulose carbamates. *Polymer Degradation and Stability*, *70*(3). https://doi.org/10.1016/S0141-3910(00)00119-1

NASDAQ. (2019, July 22). Global Viscose Fiber Industry Outlook to 2025 with Focus on the Chinese Market - Trends, Supply, Capacity, Competition Pattern, Policies, Import,

Export, and Prices. *NASDAQ OMX's News Release Distribution Channel*. https://ezproxy.cc.lut.fi/wire-feeds/global-viscose-fiber-industry-outlook-2025-with/docview/2260948447/se-2?accountid=27292

Nayak, R. (2022). Sustainable Fibres for Fashion and Textile Manufacturing. *Sustainable Fibres for Fashion and Textile Manufacturing*, 15. https://doi.org/10.1016/C2020-0-01486-6

Nozawa, Y., & Higashide, F. (1981). Partially carbamate reaction of cellulose with urea. In *Journal of Applied Polymer Science* (Vol. 26, Issue 6). https://doi.org/10.1002/app.1981.070260633

Olsson, C., & Westman, G. (2013). Direct Dissolution of Cellulose: Background, Means and Applications. *Cellulose - Fundamental Aspects*. https://doi.org/10.5772/52144

Paunonen, S., Kamppuri, T., Katajainen, L., Hohenthal, C., Heikkilä, P., & Harlin, A. (2019). Environmental impact of cellulose carbamate fibers from chemically recycled cotton. *Journal of Cleaner Production*, *222*, 871–881. https://doi.org/10.1016/J.JCLEPRO.2019.03.063

Perkin Elmer Inc. (2012). *The Effects of Varying Force and Contact on ATR Spectra*. 4–6.

Potthast, A., Rosenau, T., & Kosma, P. (2006). Analysis of oxidized functionalities in cellulose. In *Advances in Polymer Science* (Vol. 205, Issue 1). https://doi.org/10.1007/12_099

Pöyry Finland Oy. (2018). *KaiCell Fibers Oy Paltamon biojalostamo - Ympäristövaikutusten arviointiselostus*.

Redemann, C. E., Riesenfeld, F. C., & La Viola, F. S. (1958). Formation of Biuret from Urea. *Industrial and Engineering Chemistry*, *50*(4), 633–636. https://doi.org/10.1021/IE50580A035/ASSET/IE50580A035.FP.PNG_V03

Roberts, J. M., & Liu, Y. (2019). Solubility and solution-phase chemistry of isocyanic acid, methyl isocyanate, and cyanogen halides. *Atmos. Chem. Phys*, *19*, 4419–4437. https://doi.org/10.5194/acp-19-4419-2019

Saxell, H., Rantamäki, P., & Ekman, K. (2014). *METHOD FOR MAKING CELLULOSE CARBAMATE* (EP 3 161 009 B1). https://data.epo.org/publication-

server/document?iDocId=6305387&iFormat=0

Sayyed, A. J., Deshmukh, N. A., & Pinjari, D. V. (2019). A critical review of manufacturing processes used in regenerated cellulosic fibres: viscose, cellulose acetate, cuprammonium, LiCl/DMAc, ionic liquids, and NMMO based lyocell. *Cellulose*, *26*(5), 2913–2940. https://doi.org/10.1007/S10570-019-02318-Y/FIGURES/8

Schaber, P. M., Colson, J., Higgins, S., Thielen, D., Anspach, B., & Brauer, J. (2004). Thermal decomposition (pyrolysis) of urea in an open reaction vessel. *Thermochimica Acta*, *424*, 131–142. https://doi.org/10.1016/j.tca.2004.05.018

Shabbir, M. (Ed.). (2023). *Regenerated Cellulose and Composites*. https://doi.org/10.1007/978-981-99-1655-9

Sixta, H. (2008). Handbook of Pulp. In *Handbook of Pulp* (Vols. 1–2). https://doi.org/10.1002/9783527619887

Sun, S., Foster, T. J., Macnaughtan, W., Mitchell, J. R., Fenn, D., Koschella, A., & Heinze, T. (2009). Self-association of cellulose ethers with random and regioselective distribution of substitution. *Journal of Polymer Science Part B: Polymer Physics*, *47*(18), 1743–1752. https://doi.org/10.1002/POLB.21775

Suomen Tekstiili & Muoti. (2021). *6 Textile Fibre Innovations – Leading the Textile Industry Revolution - Suomen Tekstiili & Muoti*. Fablehti.Fi 12/21. https://www.stjm.fi/fabmedia/tulevaisuus/6-textile-fibre-innovations-leading-the-textile-industry-revolution/

Textile Exchange. (2023). *Distribution of manmade cellulosic fibers (MMCFs) production worldwide in 2022, by type*. Statista. Statista Inc.

Vo, L. T. T., Hajji, F., Široká, B., Manian, A. P., Davis, A., Foster, T. J., & Bechtold, T. (2014). Direct carbamation of cellulose fiber sheets. *Cellulose*, *21*(1). https://doi.org/10.1007/s10570-013-0116-z

Vo, L. T. T., Široká, B., Manian, A. P., & Bechtold, T. (2010). Functionalisation of cellulosic substrates by a facile solventless method of introducing carbamate groups. *Carbohydrate Polymers*, *82*(4). https://doi.org/10.1016/j.carbpol.2010.06.052

Waleed, H. Q., Csécsi, M., Hadjadj, R., Thangaraj, R., Pecsmány, D., Owen, M., Szőri, M., Fejes, Z., Viskolcz, B., & Fiser, B. (2022). Computational study of catalytic urethane formation. *Polymers*, *14*(1). https://doi.org/10.3390/polym14010008

Wei, Y., Zhou, M., Yao, A., & Zhu, P. (2020). Preparation of microfibrillated cellulose from wood pulp through carbamate modification and colloid milling. *Applied Sciences (Switzerland)*, *10*(6). https://doi.org/10.3390/APP10061977

Wertz, J. L., Bédué, O., & Mercier, J. P. (2010). Cellulose science and technology. In *Cellulose Science and Technology*. https://doi.org/10.1201/b16496

Willberg-Keyriläinen, P., Hiltunen, J., & Ropponen, J. (2018). Production of cellulose carbamate using urea-based deep eutectic solvents. *Cellulose*, *25*(1). https://doi.org/10.1007/s10570-017-1465-9

Woodings, C. (2001). *Regenerated cellulose fibres*. 187.

Xiong, L. K., Yu, G. M., & Yin, C. Y. (2017). Synthesis and characterization of cellulose carbamate by liquid-solid phase method. *Fibers and Polymers*, *18*(1). https://doi.org/10.1007/s12221-017-5758-2

Xu, D., Shang, J., Wang, J., Li, Y., Peng, Y., Li, X., & Zhou, J. (2023). Effect of hemicellulose content on the solution properties of cellulose carbamates in NaOH/ZnO aqueous system. *International Journal of Biological Macromolecules*. https://doi.org/10.1016/j.ijbiomac.2023.125649

Xu, M., Li, T., Zhang, S., Li, W., He, J., & Yin, C. (2021). Preparation and characterization of cellulose carbamate membrane with high strength and transparency. *Journal of Applied Polymer Science*, *138*(12). https://doi.org/10.1002/app.50068

Yalkowsky, S. H. (Samuel H., He, Y., & Jain, P. (2010). *Handbook of aqueous solubility data*. 1608.

Yin, C., & Shen, X. (2007). Synthesis of cellulose carbamate by supercritical CO2-assisted impregnation: Structure and rheological properties. *European Polymer Journal*, *43*(5). https://doi.org/10.1016/j.eurpolymj.2007.01.041

Yu, G., Teng, Y., Fu, Y., & Yin, C. (2017). Preparation of Cellulose Carbamates and

Applications of Their Regenerated Membranes. *Gaofenzi Cailiao Kexue Yu Gongcheng/Polymeric Materials Science and Engineering*, *33*(9). https://doi.org/10.16865/j.cnki.1000-7555.2017.09.026

Zhang, Y., Yin, C., Zhang, Y., & Wu, H. (2013). Synthesis and characterization of cellulose carbamate from wood pulp, Assisted by supercritical carbon dioxide. *BioResources*, *8*(1). https://doi.org/10.15376/biores.8.1.1398-1408

Zhu, N., Qian, F., Xu, X., Wang, M., & Teng, Q. (2021). Thermogravimetric experiment of urea at constant temperatures. *Materials*, *14*(20). https://doi.org/10.3390/ma14206190

Appendix 1. Measurement data

Hot press

Name of experiment	Temperature of the plates, [°C]	Pressing time, [min]	Urea concentration in impregnation, [%]	Final temperature, [°C]	Nitrogen content, [%]	Nitrogen content stdev, [%]	CED viscosity, [ml/g]
HP1	190	1	4	165	0.10	0.01	-
HP2	170	1	4	155	0.08	0.00	-
HP3	190	3	4	184	0.23	0.01	-
HP4	170	3	4	170	0.13	0.00	161
HP5	190	1	8	150	0.09	0.00	165
HP6	170	1	8	140	0.10	0.01	166
HP7	190	3	8	180	0.25	0.00	158
HP8	170	3	8	168	0.19	0.01	167

Name of experiment	Mass of starting sheet, [g]	Mass after impregnation, [g]	Urea dose per dry cellulose, [%]	Yield, [%]	L*	a*	b*
HP1	507.9	868.1	3.31	12.94	-	-	-
HP2	511.2	872.9	3.30	10.37	-	-	-
HP3	503.1	862.2	3.33	29.58	86.20	1.61	12.15
HP4	513.3	876.2	3.30	16.86	-	-	-
HP5	512.6	880.5	6.69	7.58	90.45	-0.71	4.04
HP6	505.9	878.7	6.85	6.25	-	-	-
HP7	504.0	880.0	6.93	15.45	84.60	1.03	10.30
HP8	504.7	882.5	6.95	11.71	-	-	-

Closed reactor

Sample code	Urea dose, [%]	Drying time, [min]	DMC, [%]	DMC stdev, [%]	Nitrogen, content, [%]	Nitrogen content stdev, [%]	Yield, [%]	CED viscosity, [ml/g]
ND1	4	105	88.9	4.73	0.19	0	20.55	320
ND2	4	30	42.9	3.89	0.09	0.01	9.73	343
ND3	4	0	36.2	0.28	0.08	0	8.65	371
ND4	20	105	86.2	2.55	0.34	0	7.36	287
ND5	20	30	45.2	0.92	0.13	0	2.81	332
ND6	20	0	37.8	0.21	0.10	0	2.16	352
D1	4	105	98.3	1.20	0.13	0	14.06	597
D2	4	70	83.1	6.93	0.31	0	33.53	317
D3	4	0	45.6	0.21	0.51	0.01	55.16	310
D4	20	105	95.9	0.21	0.07	0.01	1.51	463
D5	20	70	85.3	4.10	0.16	0.02	3.46	266
D6	20	0	47.4	0.21	0.19	0	4.11	302

ND = never-dried, D= dried

Sample code	Urea dose, [%]	DMC, [%]	DMC stdev, [%]	Nitrogen, content, [%]	Nitrogen content stdev, [%]	Yield, [%]	CED viscosity, [ml/g]
SA1	4	35.3	0.07	0.10	0.01	10.82	371
SA2	20	37.3	0.64	0.13	0.01	2.81	351
SA3	4	91.8	9.33	0.21	0	22.71	293
SA4	20	91.7	4.74	0.29	0.01	6.27	276
ZC1	4			0.08	0	8.65	365
ZC2	20			0.17	0.01	3.68	348
ZC3	4	78.2	8.63	0.33	0	35.69	267
ZC4	20	79.6	1.91	0.35	0.01	7.57	243
ZS1	4	35.5	0.14	0.08	0.01	8.65	361
ZS2	20	38.4	0.49	0.13	0	2.81	336
ZS3	4	95.6	1.77	0.20	0	21.63	759
ZS4	20	89.8	1.697056	0.43	0.01	9.30	251

SA = sodium acetate, ZC = zinc chloride, ZS = zinc sulphate

Sample code	L*	a*	b*
B	96.35	0.44	7.25
C	90.90	-1.03	3.54
HP3	86.20	1.61	12.15
HP5	90.45	-0.71	4.04
HP7	84.60	1.03	10.30
ND1	68.20	4.57	15.20
ND2	79.05	3.77	14.85
ND3	82.60	3.10	13.30
ND4	74.15	4.70	16.50
ND5	81.55	3.44	14.40
ND6	84.00	2.92	12.60
D1	90.85	0.32	7.10
D2	75.10	4.36	15.35
D3	78.95	3.31	13.90
D4	86.00	3.16	13.35
D5	75.25	4.33	16.05
D6	80.85	2.85	13.35
SA1	83.00	3.14	13.70
SA2	82.70	2.96	13.60
SA3	69.30	5.10	16.70
SA4	74.30	5.12	18.10
ZC1	81.70	3.85	14.70
ZC2	70.20	6.33	19.20
ZC3	51.30	8.66	21.40
ZC4	57.00	9.71	23.40
ZS1	80.10	3.78	14.60
ZS2	70.60	5.75	18.50
ZS3	83.20	2.77	11.20
ZS4	55.70	8.56	21.70

	Peak intensity 1704	Peak intensity 1623	Peak ratio	Number of parallel measurements
ND1	0.234	0.317	0.738	4
ND2	0.091	0.265	0.342	2
ND3	0.153	0.391	0.390	4
ND4	0.369	0.370	0.996	2
ND5	0.185	0.628	0.295	4
ND6	0.165	0.431	0.383	2
D1	0.227	0.569	0.399	2

D2	0.509	0.528	0.963	2
D3	0.642	0.481	1.335	4
D4	0.227	0.637	0.356	2
D5	0.437	0.464	0.942	4
D6	0.443	0.470	0.941	4
SA1	0.087	0.379	0.229	2
SA2	0.078	0.224	0.350	2
SA3	0.437	0.598	0.730	2
SA4	1.373	1.524	0.901	4
ZC1	0.060	0.223	0.268	2
ZC2	0.751	0.901	0.833	4
ZC3	1.239	1.454	0.852	4
ZC4	0.875	1.090	0.803	4
ZS1	0.067	0.174	0.384	2
ZS2	0.059	0.133	0.439	2
ZS3	1.183	1.185	0.998	4
ZS4	1.001	1.219	0.821	4

Appendix 2. Main effects plots for L*, a* and b*

*Main effects plot for ΔL**

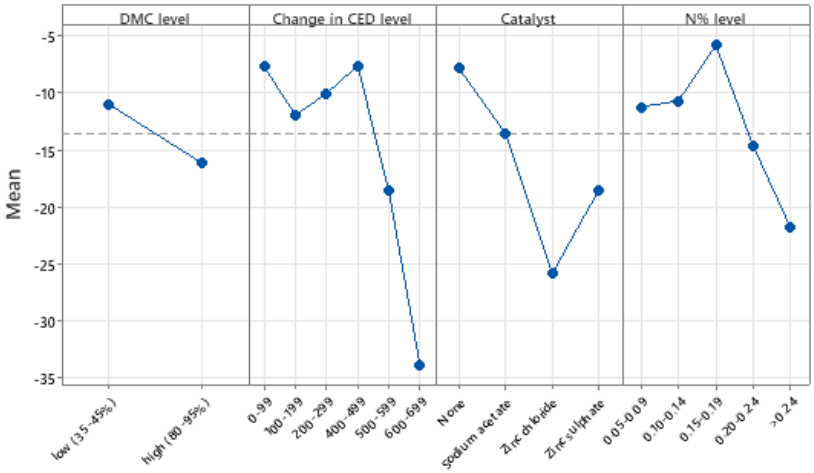

*Main effects plot for Δa**

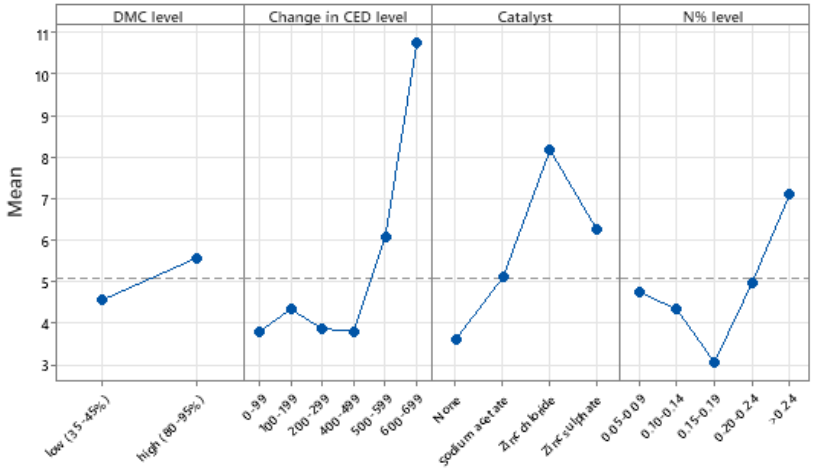

*Main effects plot for Δb**

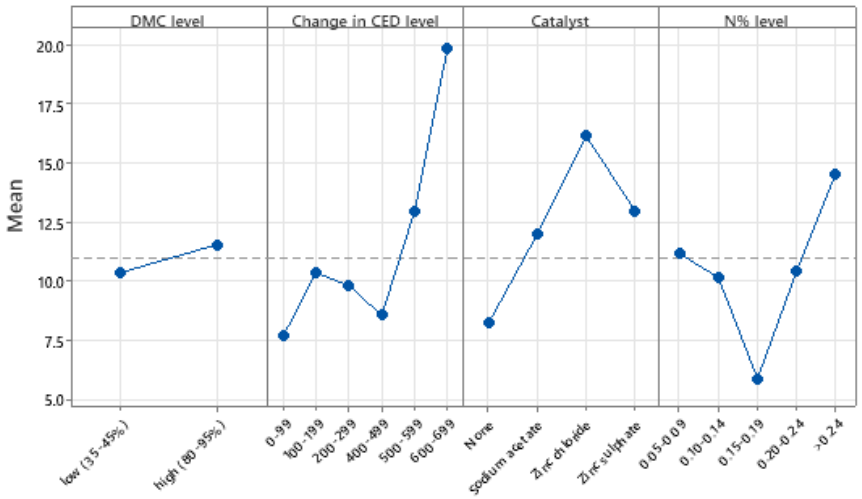

Appendix 3. Regression models

HOT PRESS

Coded Coefficients

Term	Effect	Coef	SE Coef	T-Value	P-Value	VIF
Constant		0,1462	0,0112	13,00	0,000	
Temp	0,0425	0,0213	0,0112	1,89	0,132	1,00
Time	0,1075	0,0537	0,0112	4,78	0,009	1,00
Urea	0,0225	0,0113	0,0112	1,00	0,374	1,00

Model Summary

S	R-sq	R-sq(adj)	R-sq(pred)
0,0318198	87,26%	77,70%	49,04%

Analysis of Variance

Source	DF	Adj SS	Adj MS	F-Value	P-Value
Model	3	0,027738	0,009246	9,13	0,029
Linear	3	0,027738	0,009246	9,13	0,029
Temp	1	0,003613	0,003613	3,57	0,132
Time	1	0,023113	0,023113	22,83	0,009
Urea	1	0,001013	0,001013	1,00	0,374
Error	4	0,004050	0,001012		
Total	7	0,031788			

Regression Equation in Uncoded Units

N% = -0,378 + 0,00213 Temp + 0,0537 Time
+ 0,00563 Urea

FTIR-ATR

The regression equation is
N% = - 0.03117 + 0.3554 peak ratio

Model Summary

S	R-sq	R-sq(adj)
0.0611696	82.37%	81.85%

Analysis of Variance

Source	DF	SS	MS	F	P
Regression	1	0.594504	0.594504	158.89	0.000
Error	34	0.127219	0.003742		
Total	35	0.721722			